Towards the coupling of a chemical transport model with a micro-scale Lagrangian modelling system for evaluation of urban NO_x levels in a European hotspot

Giorgio Veratti[1], Sara Fabbi[1], Alessandro Bigi[1], Aurelia Lupascu[2], Gianni Tinarelli[3], Sergio Teggi[1], Giuseppe Brusasca[3], Tim M. Butler[2] and Grazia Ghermandi[1]

[1]Department of Engineering "Enzo Ferrari", University of Modena and Reggio Emilia, via Pietro Vivarelli 10, 41125 Modena, Italy
[2]Institute for Advanced Sustainability Studies, Helmholtzstraße 5, 14467 Potsdam, Germany
[3]ARIANET S.r.l., via Gilino 9, 20128 Milano, Italy

Correspondence to: Giorgio Veratti (giorgio.veratti@unimore.it)

Abstract. A multi-scale modelling system was developed to provide hourly NO_x concentration fields at a building-resolving scale in the urban area of Modena, a city in the middle of the Po Valley (Italy), one of the most polluted areas in Europe. The WRF-Chem model was applied over three nested domains and employed with the aim of reproducing local background concentrations, taking into account meteorological and chemical transformation at the regional scale with nested resolutions of 15 km, 3 km and 1 km. Conversely, the PMSS modelling system was applied to simulate 3D air pollutant dispersion, due to traffic emissions, with a very high-resolution (4 m) on a 6 km x 6 km domain covering the city of Modena.

The methodology employed to account for anthropogenic emissions relies on two different strategies. Traffic emissions were based on a bottom-up approach using emission factors suggested by the European Environmental Agency with traffic fluxes estimated by the PTV VISUM model in the urban area of Modena, combined with direct traffic flow measurements performed between October 28 and November 8, 2016 which was used for the hourly vehicle modulation. Other anthropogenic emissions were taken from the TNO-MACC III inventory at the scales resolved by the WRF-Chem model. Simulations were performed for the same period whereby the traffic measurement campaign was carried out.

2 m temperature and 10 m wind speed were captured quite well by the WRF-Chem model with statistical metrics in line with similar case studies related to the Northern Italy. The NO_x concentrations reproduced in the Po Valley area by WRF-Chem were on average simulated reasonably well with a general negative bias in almost all the examined rural background monitoring stations. Additionally, the deployment of an emission inventory at the original resolution (7 km) highlighted that increasing resolution from 3 km to 1 km does not generally improve the model performance.

Nevertheless, simulated and observed NO_x hourly concentrations in the urban area of Modena exhibit a large agreement in particular for urban traffic site where detailed traffic emission estimations proved to be very successful in reproducing the observed NO_x trend. At urban background stations, despite a general underestimation of the observed concentrations, the combination of WRF-Chem with PMSS provided daily pattern in line with observations. The analysis of the modelled NO_x daily cycle pointed out also that at both traffic and background urban stations the morning NO_x peak concentration was on

average underestimated. This could be explained with an overestimation of mixing phenomena between 07:30 a.m. and 10:00 a.m. by WRF-Chem which leads to a greater dispersion of NO_x along the vertical and thus a morning underestimation. The statistical analysis showed finally that PMSS combined with WRF-Chem at both the resolutions (3 km and 1 km) and at both traffic and background sites fulfilled standard acceptance criteria for urban dispersion model evaluation, confirming that the proposed multi-modelling system can be employed as a tool to support environmental policies, epidemiological studies and urban mobility planning.
Keywords: WRF-Chem, PMSS modelling system, Multi-model approach, Traffic emissions, Modena.

1 Introduction

Atmospheric pollution is one of the main risk factors for a number of pollution-related diseases and health conditions: they may occur through the appearance of harmful and carcinogenic effects on the respiratory system as well as the onset of other cardiovascular, nervous and ocular pathologies (Loomis et al., 2013, Novaes et al., 2010, PopeIII et al., 2003). These critical issues particularly affect urban areas with a higher population density: a complex mixture of pollutants is produced by inefficient combustion of fuels in internal combustion engines, power generation and other human activities like domestic heating and cooking.

One of the most critical air pollutants in terms of health effects is nitrogen dioxide (NO_2), whose levels in the last years exceeded national and WHO standards in many urban areas across Europe (European Environment Agency, 2016). In Italy, and more particularly in the Po Valley, despite an overall decrease in PM in the last 10 years (Bigi and Ghermandi, 2016), the urban population is still exposed to harmful levels of NO_2.

The present research has as its goal the estimation of the air quality in the urban area of Modena, a city in the central Po Valley, in terms of NO_x atmospheric concentrations. More in detail, the aim of the project is to support environmental policies, epidemiological studies and urban planning and management.

Current approaches to produce spatial maps of urban air pollution include the use of interpolation methods and land-use regression (LUR) models. However, all these techniques need a large number of in-situ observations at strategic locations to represent the full spatial and temporal pollutant variability and cannot be used to take into account turbulent atmospheric dispersion. To meet this need, a variety of micro (Moussafir et al, 2004, Öttl, 2015) and local (Tinarelli et al, 1992, Bellasio and Bianconi, 2012, Cimorelli et al, 2004) scale air dispersion models have been developed in the last few years, as they can provide a high-resolution information on air pollution level within urban city area by taking into account space-time emissions distribution and local meteorological characteristics (Ghermandi et al, 2014, Ghermandi et al, 2015).

A key issue is the quantitative estimation of the different contribution to air pollution level from emissions sources located within the city urban environment and from countryside areas, also known as rural background. An approach that has been used for several years to account for both urban and rural contribution is generally called “Lenschow” approach (Lenschow et al., 2001), which envisages the influence of a city as the difference between the concentrations in the urban environment

and the concentrations at rural site. This methodology is generally applied in source apportionment studies in order to estimate the primary and secondary component of PM by means of receptors models (Pirovano et al., 2015, Bove et al., 2014), or in urban impact assessments through an approach combining measurements and modelling results. In this latter case, the model is used to evaluate the contribution (effects) of the sources located within the city, while measured background concentrations are added to the simulated concentrations to account for remote sources outside the simulation domain (Ghermandi et al. 2019, Berchet et al., 2017).

Despite the flexibility in enforcing measured-based activity and modelling results, a number of criticisms related to the applicability of this methodology were recently highlighted. Following Thunis (2018) the city urban impact can be defined as the sum of three components: the Lenschow urban increment, which is the concentration difference between the city and background locations, the "city spread" meaning the impact of the city at the rural background location, and the "background deviation" that quantifies the concentration difference between city and background location when city emissions are set equal to zero. According to this definition, the "Lenschow" approach can be correctly employed only when the "city spread" and the "background deviation" are negligible or compensate each other, i.e. the urban impact in background area is close to zero and when background levels are spatially homogenous.

An alternative approach to quantify the different contributions to air pollution in the city is based on Chemical Transport Models (CTMs) which, unlike the Lenschow incremental approach, are able to generate different emission scenarios on multi spatial scale, from regional to local, which can be exploited to estimate background concentrations keeping city emissions set to zero.

Based on the advantages given by CTMs, the methodology employed in this study was a modelling activity relied on the NO_x dispersion by combining two different models: the Weather Research and Forecasting (WRF) model coupled with Chemistry (Grell et al., 2005), which is able to compute concentrations fields over regional domain by considering specific emission scenarios, and the Parallel Micro SWIFT and SPRAY (PMSS, Moussafir et al., 2013, Oldrini et al., 2017) modelling suite accounting for dispersion phenomena within the urban area.

In this project, the PMSS modelling suite was used to simulate at building-scale resolution the NO_x dispersion produced by urban traffic flows in the city of Modena. Conversely, the WRF-Chem model simulations were performed to estimate the NO_x background concentrations on multiple domains with a nesting technique, in order to take into account emissions both at regional and local scale by excluding traffic emissions sources over the city of Modena. A similar approach was used also by Tewari et al. (2010), Wyszogrodzki et al. (2012) and Kwak et al. (2015), which developed an integrated urban air quality modelling system by coupling a CFD model with a chemical transport model in order to account not only the dispersion in buil-up areas but also to consider larger scale influences.

In the first part of the paper the modelling system which is applied to take into account both urban and background emissions sources is described. The following section describes the set-up of the models employed in the simulation, along with the method for estimation of emissions. Finally, the performance of the models in representing the meteorological mesoscale reconstruction and the pollutant dispersion is evaluated.

2 Materials and method

2.1 Modelling chain description

With the aim of providing hourly NO_x concentration maps over the urban area of Modena, a hybrid modelling system composed by WRF-Chem, an Eulerian model and PMSS, a Lagrangian particle dispersion model, was employed in this study. The choice of this modelling chain was based on the WRF-Chem ability to simulate the emissions, transport and chemical transformations simultaneously with meteorology at large scale, and on the PMSS capability to provide high resolution air quality maps over an entire urban domain characterized by large spatial and temporal concentrations gradient, with a reasonable computation time (Ghermandi et al., 2015).

Figure 1 illustrates the interplay between WRF-Chem and PMSS. The WRF-Chem model was used to estimate NO_x concentrations on multiple domains at different grid resolutions spanning from the European domain to the Po Valley area with a nesting technique, necessary to take into account emissions at regional scale that can affect urban air quality in Modena. Then, wind streams within the city were determined by a cascade of scales from global to buildings level: synoptic and local scale meteorological conditions in the region surrounding the city of Modena were simulated by WRF-Chem taking into account the local topography and land-use data. Driven by these mesoscale flow patterns, high resolution winds were computed in the city to account for buildings and street canyons by performing the diagnostic mass-consistent Parallel-Micro-SWIFT model. Secondly, Lagrangian dispersion simulations driven by high resolution winds were carried out with Parallel-Micro-SPRAY by estimating urban traffic emission flows. As a final step of the procedure, NO_x traffic urban concentrations, simulated with Parallel-Micro-SPRAY, were added to NO_x background concentrations estimated with the WRF-Chem model. Further explanations regarding the methodology used to avoid double counting of traffic emissions within Modena urban domain are reported in section 2.5.

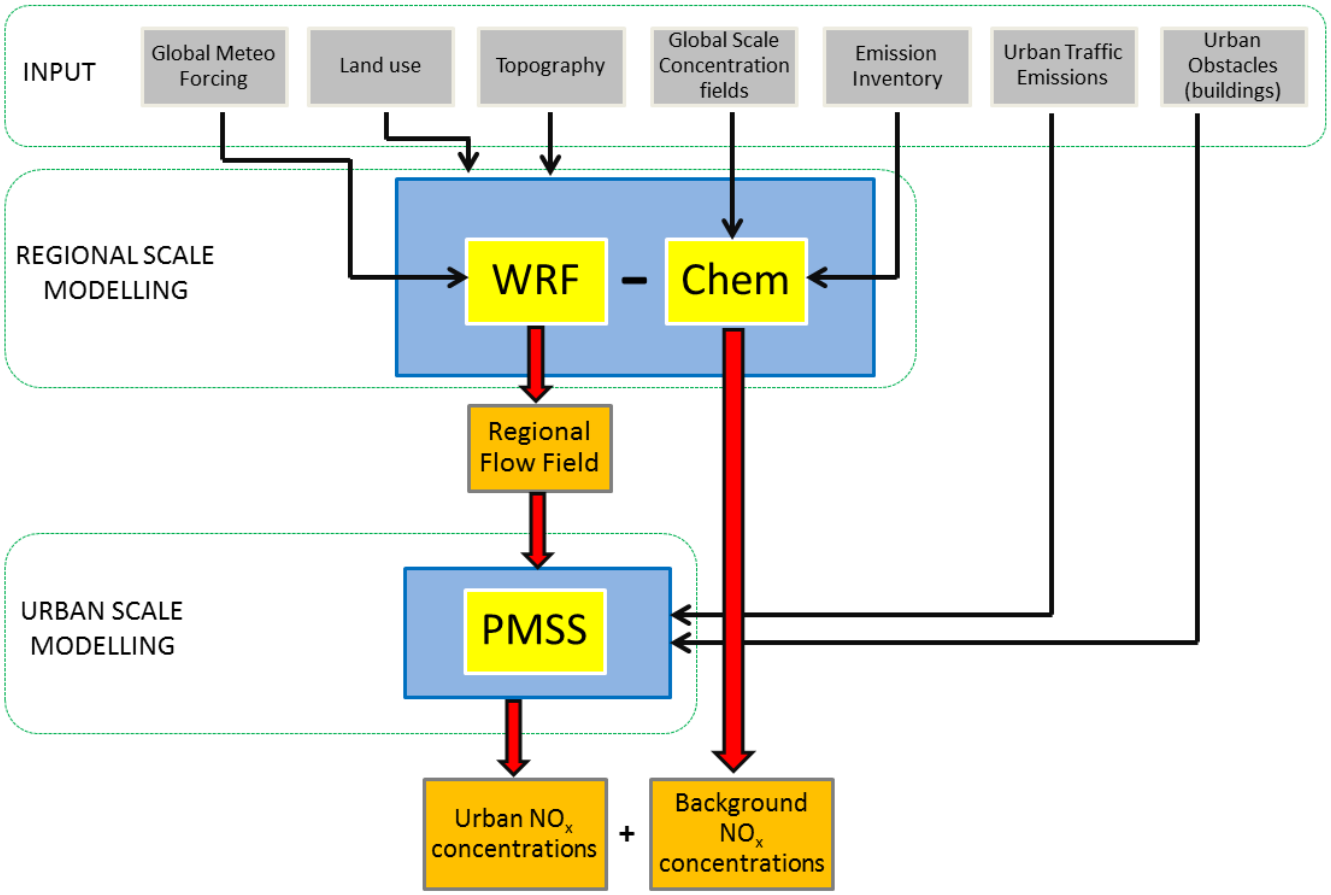

Figure 1: Outline of the multi-model approach implemented to generate hourly NO_x concentrations fields**.**

2.2 WRF-Chem Set-up

For this application, the Weather Research and Forecasting model with chemistry (WRF-Chem), version 3.9.1, was applied over three one-way nested domains, centred in the urban area of Modena. The outer domain (d01) covers most of Europe with 150 x 150 grid cells at 15 km horizontal resolution, the intermediate domain (d02) covers the North of Italy with a resolution of 3 km (150 x 150 grid cells) and the innermost domain (d03) focuses on the Po Valley area with a spatial resolution of 1 km with 175 x 175 grid cells (Figure 2). The model was configured with 35 vertical levels with the first layer approximately at 30 m and the model top set at 50 hPa.

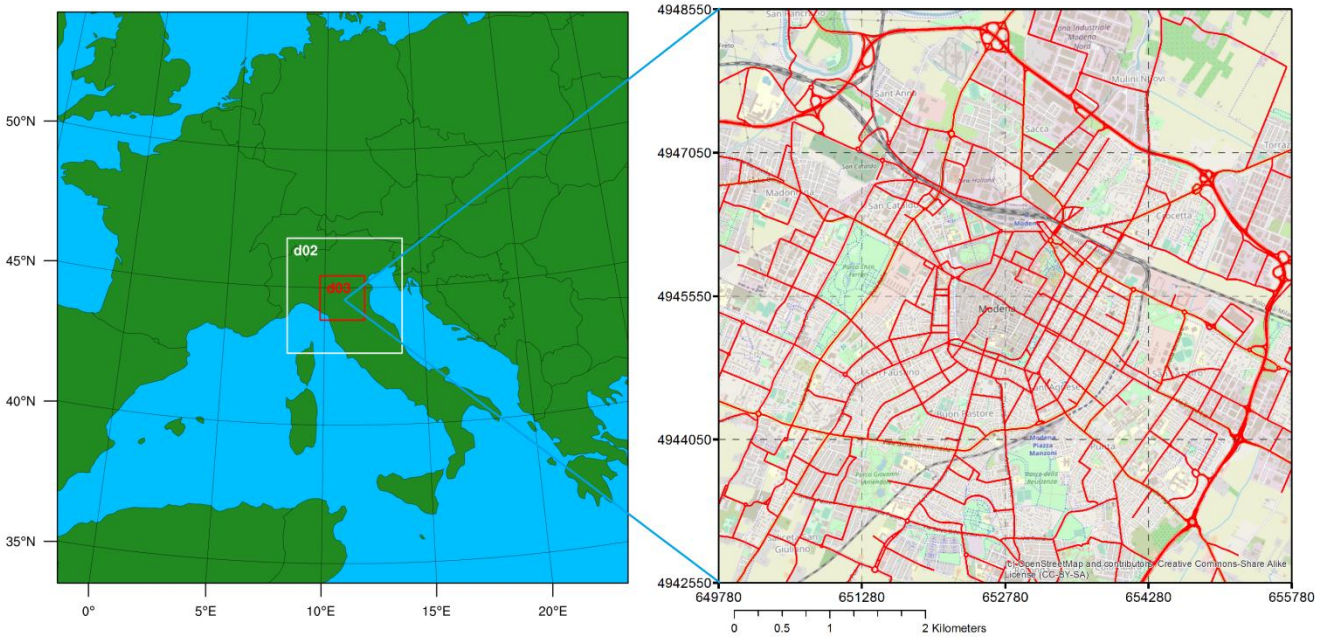

Figure 2: Overview of the WRF-Chem model domains on the left (Geographic coordinate system-WGS84) and PMSS investigation domain with the considered Modena street network represented as red lines on the right (UTM32-WGS84).

The main options for physical and chemical schemes adopted here are reported in Table 1. These include the Noah Land Surface Model (Chen and Dudhia, 2001), the Yonsei University Planetary Boundary Layer scheme (Hong S.-Y., 2010), the Grell-Freitas cumulus parameterization (Grell and Freitas, 2014) activated only for the outer domain, the Lin microphysics scheme (Lin et al., 1983), and the Rapid Radiative Transfer Model (RRTM) radiation scheme (Mlawer et al., 1997) aimed to represent both shortwave and longwave radiation.

Table 1: WRF-Chem model parameterisation.

Process	WRF-Chem option
Land-surface model	Noah Land Surface Model
Boundary layer scheme	YSU
Cumulus parameterization	Grell-Freitas (only for the outer domain)
Microphysics	Lin
Short-wave radiation	RRTM with MCICA method
Long-wave radiation	RRTM with MCICA method
Gas-phase mechanism	MOZART
Aerosol model	MOSAIC 4 bins

The MOZART gas-phase chemical mechanism developed by Emmons et al. (2010), and the MOSAIC aerosol model (Zaveri et al. 2008) were used to simulate airborne pollutants over the nested domains. The first one includes 85 chemical species, 196 reactions and is consistent with the chemistry used in the global model that provides the chemical input and boundary conditions for the nested simulations. MOSAIC uses a sectional bin approach for the representation of the aerosol size distribution. The MOSAIC model predicts several aerosol species, such as sulfate, nitrate, ammonium, elemental carbon, and primary aerosols (POAs). Processes involving secondary organic aerosols (SOAs) formation were represented by the scheme based on Hodzic and Jimenez (2011).

Meteorological initial and boundary conditions were provided by the 6-hourly ECMWF analysis field (ERA5 dataset) with a horizontal resolution of 0.25° x 0.25°, interpolated to 37 pressure levels from 1000 to 1 hPa. Data included 3D fields of temperature, specific humidity and wind speed components. 2D surface parameters such as mean sea level pressure, sea surface temperature, soil temperature and volumetric soil water content were also considered. A grid nudging on temperature and wind field has been also performed within the boundary layer in all three model configurations using as input data the ECMWF analysis.

As to land use, the Corine Land Cover (CLC) dataset was adopted after reclassifying it into the 33 USGS classes to match the WRF land use tables. Chemical initial and boundary conditions were provided by the global Model for OZone And Related chemical Tracers output (MOZART-4; Emmons et al., 2010). Biogenic emissions were calculated online by the Model of Emissions of Gases and Aerosols from Nature version 2.1 (MEGAN2.1) by Guenther et al. (2012). In addition, sea salt and dust emissions are calculated online.

2.3 PMSS modelling system description

Parallel Micro SWIFT SPRAY or PMSS (Oldrini et al. 2011, 2017) is the parallelized version of the MSS modelling suite (Tinarelli et al. 2007, 2013) constituted by the individual models SWIFT and SPRAY, both used in small scale urban model (a.k.a. Micro-SWIFT and Micro-SPRAY).

Micro-SWIFT is a 3D mass-consistent diagnostic model that uses terrain-following coordinates to provide diagnostic wind, turbulence, temperature and humidity fields using data from a dispersed meteorological network.

The first step performed by Micro-SWIFT is the interpolation of the heterogeneous meteorological input data, such as surface and vertical measurements profile or regional meteorological model output, to reconstruct the 3D wind field. Then, the first computed wind field is modified in the zones around isolated or group of buildings following the approach suggested by Röckle (1990) and Kaplan and Dinar (1996) adopting a parametrization of the recirculating flow regions around, behind, over and between obstacles. Subsequently, the mass conservation constraint is imposed through the impermeability conditions on the ground and at building surfaces. Finally, a RANS flow solver can be optionally used to simulate more accurate velocity and pressure fields in built-up environments than obtained with the pure diagnostic flow model configuration. With the RANS approach, the momentum equation is introduced in the computation and the turbulent Reynolds stress tensor is modelled by a zero-order closure based on mixing-length theory and the momentum and pressure equations are solved using the fractional time step technique (Gowardhan et al., 2011).

The estimation of the turbulence needed by Micro-SPRAY to drive pollutants dispersion is diagnosed by Micro-SWIFT through the superimposition of the background turbulence, obtained by standard boundary layer parameterizations (Hanna et al., 1982) and the turbulence inside the flow zones modified by the obstacles.

Micro-SPRAY is a 3D Lagrangian Particle Dispersion Model (LPDM) (Rodean, 1996) able to simulate the advection and the diffusion of gaseous species or fine aerosol by accounting for the presence of obstacles. The dispersion of an airborne contaminant is modelled by virtual particles that follow the turbulent motion of the air as passive tracers and their spatial distribution at a certain time represents the concentration of an emitted substance.

The trajectories of the particles emitted by a source are obtained by integrating in time their velocity. This can be considered as the sum of a transport component, defined by the local averaged wind, usually provided by Micro-SWIFT, and a stochastic component, standing for the dispersion due to the atmospheric turbulence. The stochastic component is obtained by solving a 3D form of the Langevin equation for the random velocity, following Thomson's approach (Thomson, 1987).

The PMSS modelling system has been validated (Trini Castelli et al. 2017 and 2018, Oldrini et al., 2017 and 2019) and applied (Carlino et al., 2016, Moussafir et al., 2013) to several experiments and real cases. In this study, the performances of the PMSS modelling system are exploited to estimate urban air quality in the city of Modena in a real case scenario.

2.4 PMSS set-up

A 3D wind and turbulence field and air pollution dispersion reconstruction was performed on a 6 km x 6 km square domain covering the city of Modena (Figure 2) with the PMSS modelling suite. Given the low altitude difference between different areas of the city, a flat domain was considered and a 3D reconstruction of buildings was made by using a pre-processor: 25,600 polygons contained in the ESRI shapefile (provided by Geoportale Regione Emilia-Romagna) were transformed into approximately 146,000 triangular prisms directly usable by Micro-SWIFT.

In order to guarantee both flow and pollutant dispersion fields at a high resolution in each part of the domain, a horizontal grid step of 4 m (square cells) was chosen for both Micro-SWIFT and Micro-SPRAY models. To represent the flow entering the Micro-SWIFT computational domain, vertical profiles of temperature, humidity, wind speed and direction from the innermost domain (d03) of the WRF-Chem simulation were extracted on an hourly basis. In addition, mixing height values and main background turbulence parameters (i.e. friction velocity, Monin-Obukhov length and convective scale velocity) were estimated with the Mesoscale Model Interface Program v3.4 (MMIF, https://www.epa.gov/scram/air-quality-dispersion-modeling-related-model-support-programs), which converts prognostic meteorological WRF output fields into turbulence scale parameters.

3D fields of wind, temperature and turbulence were obtained for 20 vertical levels from 3 m up to 200 m above the ground using the Micro-SWIFT model with the RANS flow solver option activated. The 2D Cressman interpolation method wind field was also considered in the configuration.

Regarding the Micro-SPRAY model simulations the horizontal grid was chosen to be identical to that of the Micro-SWIFT model computation and the vertical grid structure consisted of 10 levels with a linear progression up to 200 m above the ground level with 3 m height for the first layer close to the soil. This arrangement leads to a configuration of 1504 x 1504 x 10 nodes and a total number of $2.26 \cdot 10^7$ cells. The main SPRAY parameters also included an emissions time step of 5 seconds and a synchronisation time step of 10 seconds. Concentrations are computed every hour and sampled every 10 seconds. Since the cumulative precipitation for all the examined period was less than 10 mm, the wet deposition was not included in the set-up. The main PMSS set-up parameters are reported in Table 2.

Table 2: Micro-SWIFT and Micro-SPRAY set-up.

Micro-SWIFT		Micro-SPRAY	
Parameters	Value	Parameters	Value
Horizontal resolution	4 m	Horizontal resolution	4 m
Horizontal grid	1504 x 1504 points	Horizontal grid	1504 x 1504 points
Vertical grid	from 3 up to 200m	Vertical grid	from 3 up to 200m
	20 vertical levels		10 vertical levels

Interpolation method	Cressman 2D	Emission time step	5 s
		Averaging period for concentrations	3600 s

225
226

227 **2.5 Anthropogenic Emissions**

228 Following the regional emissions inventory database produced by Arpae Emilia-Romagna, the local environmental agency
229 (INEMAR 2013), the road traffic in Modena contributes up to the 60% of the total emissions in terms of NO_x, while the
230 domestic heating and industrial combustion represent only the 15% and 14% of the total amount. Based on this percentage
231 distribution, the methodology employed to account for anthropogenic emissions rely on two different strategies: a city-
232 tailored emission estimate, to describe traffic emissions at micro-scale resolution in the urban area of Modena, and an
233 emission inventory estimate, more suitable to account for emissions at large-scale area, used as an input for the chemical
234 transport model in order to estimate the contribution of all the SNAP (Selected Nomenclature for Air Pollution) emission
235 categories throughout Europe.
236 The anthropogenic emissions used for the parent and the nested WRF-Chem domains were taken from the TNO-MACC III
237 inventory, available on a regular grid with a horizontal resolution of 0.125° x 0.0625°, which contains emissions for air
238 pollutants such as NO_x, SO_2, NMVOC, NH_3, CO and primary particulate matter ($PM_{2.5}$ and PM_{10}). The inventory is based on
239 nationally reported emissions for specific sectors and spatially distributed with proxy data such as the population density for
240 urban emissions or the road network for non-urban emissions. The main developments with respect the version II of the
241 inventory (Kuenen et al. 2014) includes improved emissions and trends for the international sea shipping, improved wood
242 consumption estimation and more detailed spatial distribution, as well as improved industrial emissions apportioning
243 achieved through the use of CORINE land cover data instead of population density data as a default item.
244 TNO-MACC III emissions are provided as annual totals, therefore each SNAP category was scaled to take into account
245 monthly, daily variation (weekend or weekday) and hour of the day (diurnal cycle), as suggested by Kuik et al. (2018). A
246 vertical emissions distribution was also taken into account by distributing the emissions of industrial sources, airports,
247 extraction and distribution of fossil fuel into seven vertical layers, up to 750 m.
248 In order to avoid the double counting of the traffic emissions placed inside the urban area of Modena and to better represent
249 the spatial distribution of traffic sources in the nearby territory, a downscaling procedure was conducted for the SNAP
250 sectors 71-75. The original TNO dataset (resolution ca. 14 km x 7 km) covering the inner most WRF-Chem domain was
251 subdivided to a finer grid with a horizontal resolution of 1 km x 1 km.
252 Traffic fluxes of light (passenger cars and L-category vehicles) and duty (light commercial vehicle and heavy-duty trucks)
253 vehicles on the main roads of the province of Modena at morning rush hour (07:30 – 08:30, local time) for the year 2010
254 were provided by the Municipality of Modena and proceed from a simulation study by means of the PTV VISUM model

(PTV Group, Karlsruhe, Germany http://vision-traffic.ptvgroup.com/en-us/products/ptv-visum/). These data were used as a proxy variable to assign TNO-MAC III traffic emissions over the province of Modena to the portion of the land interested by PTV VISUM road network: the more traffic fluxes were estimated for a specific road segment, the more emissions were assigned to the corresponding grid (1 km x 1 km) (Figure 3**)**.

Once the downscaled grid dataset was created, a spatial surrogate function was implemented to identify the TNO-MACC III traffic emissions within the PMSS domain. This function returns zero if the territory cell is completely inside the PMSS domain, one if the territory cell is completely outside and a value between zero and one (proportional to the area outside the PMSS domain) if the territory cell crosses the domain boundaries. Finally, to exclude TNO-MACC III emissions from the PMSS domain, the spatial mask created with the surrogate function was multiplied by the downscaled traffic emission inventory.The same traffic simulation obtained with the PTV VISUM model includes also vehicle fluxes in the urban area of Modena, providing the number and the average speed for light and duty vehicles at rush hour for each segment of the urban road network, which encompasses about 1100 sections with a total length of 210 km (Figure 4**)**.

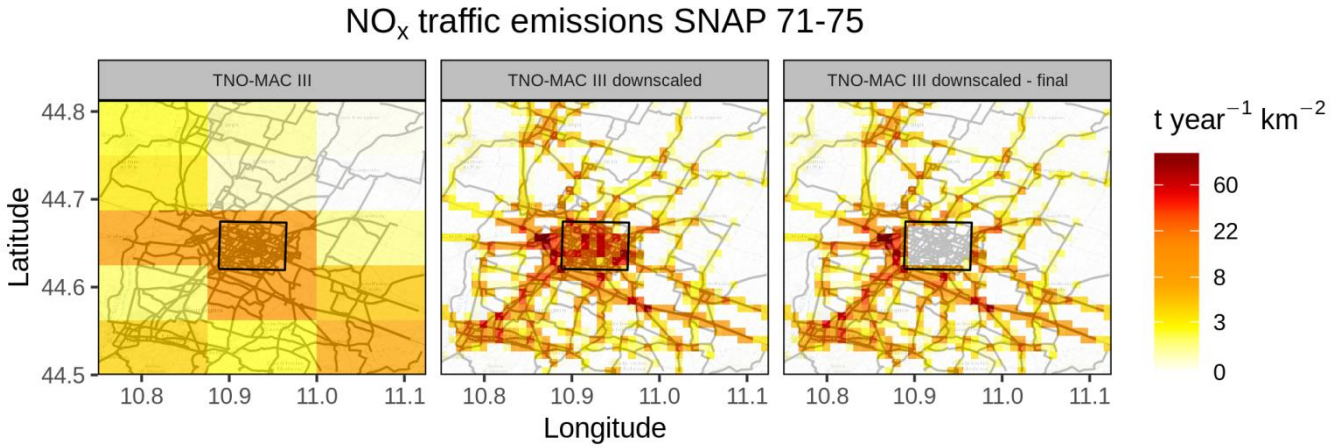

Figure 3: Total NO_x traffic emissions (SNAP sector 71-75) in the province of Modena. On the left the original TNO-MACC III inventory emissions (resolution ca. 14 km x 7 km). At the centre the TNO-MACC III inventory emissions downscaled to a resolution of 1 km x 1 km and distributed according to the street traffic flow estimated by PTV VISUM. On the right the TNO-MACC III inventory emissions downscaled to a resolution of 1 km x 1 km without the emissions by road traffic in the urban area of Modena.

The methodology chosen to estimate traffic emissions in the urban area of Modena was based on a bottom-up approach: traffic flow data simulated by PTV VISUM model were employed as “activity factor” and specific Emission Factors (EF) were used to estimate total emissions according to the fleet composition, vehicle type, fuel, engine capacity, load displacement, slope of the road, Euro emission standard and average traveling speed.

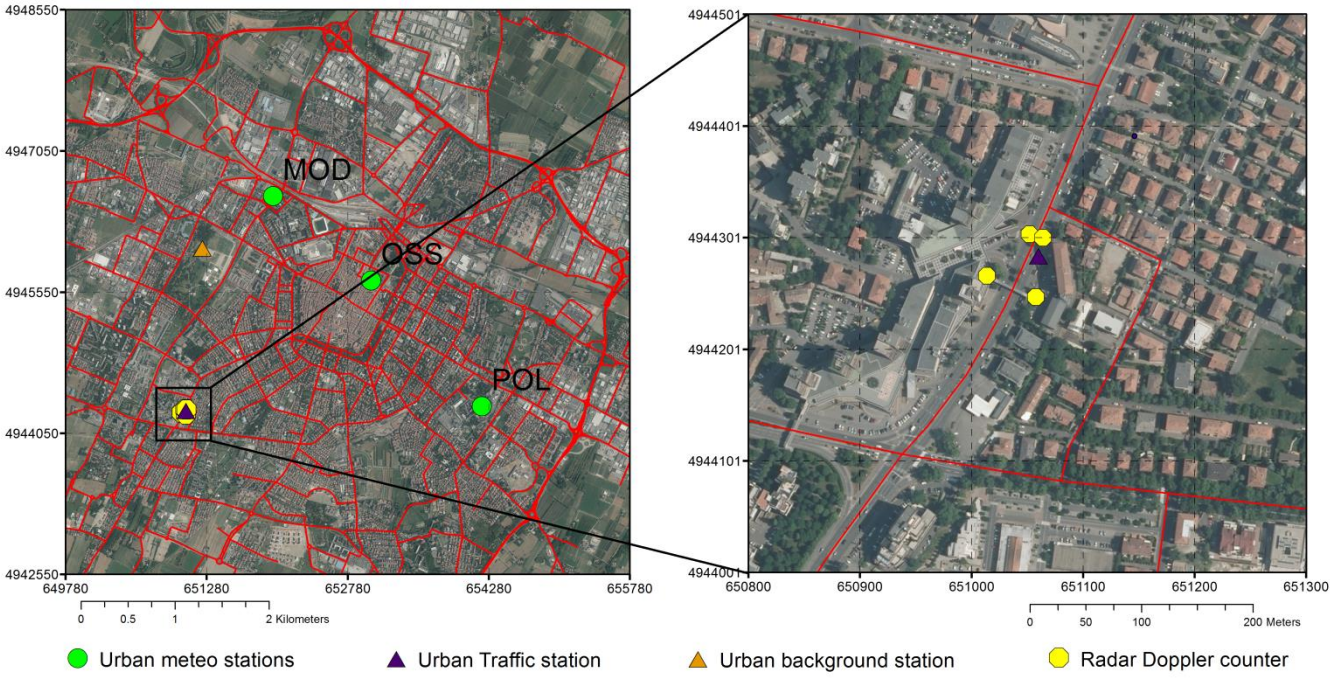

277

278 **Figure 4:** PMSS computational domain (left side) and view of the radar traffic counters position (right side). Radars are represented by
279 yellow dots, air quality urban background station by orange triangle and urban traffic station by blue triangle. Urban meteorological
280 stations are also depicted by green dots along with their label names.

281

282 With aim of estimating for each road segment the NO_x atmospheric emissions in terms of pollutant mass per trip unit, a
283 modified version of the R package VEIN (Vehicular Emissions INventories) v0.5.2 (Ibarra-Espinosa et al., 2018) was
284 employed. The latest Emission Factors suggested by Ntziachristos and Samaras (2016) were introduced in the package and a
285 series of functions to automatically compute for each road of the network the total NO_x emissions were implemented.
286 The Tier 3 methodology, defined in the European guidelines EMEP/EEA (Ntziachristos and Samaras, 2016) for the estimate
287 of exhaust emissions from road transport was adopted, and total exhaust emissions were calculated as the sum of hot
288 emissions (when the engine is at its normal operating temperature) and emissions during transient thermal engine operation
289 (termed 'cold-start' emissions). As stated before, the road network considered in the micro-scale simulation is contained in
290 the urban area of Modena, therefore only urban driving situation was considered in the emissions estimation.
291 EF values were computed for each vehicle fleet category considering the flow speed estimated by PTV VISUM, and then
292 EFs were mathematically weighted according to fleet composition to obtain for each road two EFs, one representing the light
293 vehicles and one on behalf of duty vehicles.
294 Hot emissions computation included also correction values applied to the baseline emission factors to account for different
295 vehicle age for passenger cars and light commercial vehicles, also called emissions factors degradation due to vehicle age

(Ntziachristos and Samaras, 2016). Actual average annual mileage (AAAM) for gasoline and diesel cars in the Italian vehicle stock, respectively $AAAM_{gasol}$ and $AAAM_{diesel}$, were estimated with the formulas suggested by Caserini et al. (2013). Considering *age* as the number of years between the current year and the year of vehicle purchase, the formulas can be written as follow:

$$AAAM_{gasol} = 20.817 \cdot age^2 - 1124.3 \cdot age + 15651 \qquad if\ age \leq 30\ years \tag{1}$$

$$AAAM_{gasol} = 20.817 \cdot 30^2 - 1124.3 \cdot 30 + 15651 \qquad if\ age > 30\ years \tag{2}$$

$$AAAM_{diesel} = 35.072 \cdot age^2 - 1811.2 \cdot age + 23942 \qquad if\ age \leq 30\ years \tag{3}$$

$$AAAM_{diesel} = 35.072 \cdot 30^2 - 1811.2 \cdot 30 + 23942 \qquad if\ age > 30\ years \tag{4}$$

In addition to the traffic model data, a direct vehicle flow measurement campaign was carried out continuously over two weeks between October 28 and November 8, 2016, with 4 Doppler radar counters (one for each road lane) in a four-lane road in the proximity of the intersection with the urban ring road (Ghermandi et al. 2019) (Figure 4). The radar traffic counters recorded the time, the length and the velocity for each passing vehicle. The captured vehicles were subdivided into two different groups according to the vehicle classes modelled by PTV VISUM: light vehicles, with measured length less or equal to 6 m and duty vehicles, with measured length greater than 6 m. Finally, to appropriately describe NO_x emissions under typical vehicle flux conditions, recorded flow data were used to reproduce hourly modulation rates for the entire road network.

In order to test the reliability of the hot EFs computed with the methodology previously described and to check how far these EFs are with respect the one computed considering recently emission data, based on new PEMS tests (Hausberger et al, 2019, Sjödin et al., 2018), the weighted EFs for Passenger Cars (PC), Light Commercial Vehicle (LCV), Heavy Duty Trucks (HDT) and Motorcycle in Modena were compared with the weighted average hot EFs calculated following the handbook of emission factors (HBEFA, 2019) for different European countries (Germany, Austria, Switzerland, France, Norway and Sweden).

Since the HBEFA desktop application is not available for free, an extensive analysis relied on the real vehicle fleet composition in Modena was not possible. Despite this limitation, an indicative comparison between the actual hot EFs considered in the emission computation for the city of Modena and the average hot EFs for the respective vehicles category between the 6 European countries mentioned before is shown in Figure 5. The green rectangles indicate the EFs used in study, while the red rectangles represent the average EFs computed between Germany, Austria, Switzerland, France, Norway and Sweden, when available. The black horizontal segments below and above the red rectangles upper limit indicate respectively the minimum and the maximum EF for each respective vehicle category.

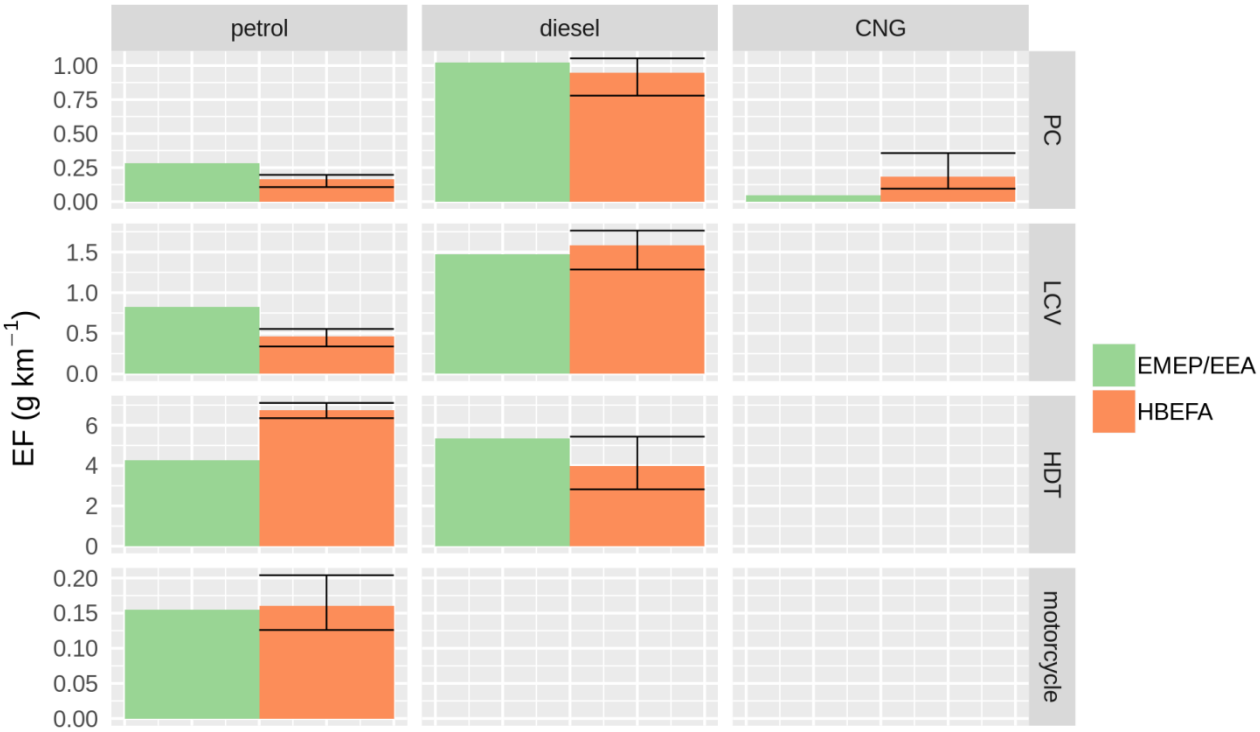

Figure 5: Comparison between weighted NO_x hot EFs used in this study, computed following the EMEP/EEA guidelines (green rectangles) and the corresponding average NO_x hot EFs computed between Germany, Austria, Switzerland, France, Norway and Sweden following the handbook of emission factors (HBEFA) version 4.1 (red rectangles). With horizontal black segment are also indicated the minimum and maximum HBEFA EF for the same six European countries. Please note the difference in the scale on the y-axis in each panel.

The hot EFs obtained following the EMEP/EEA guidelines for the city of Modena are in general in line with the hot EFs computed using the HBEFA methodology (v4.1) for similar European countries. The main differences in absolute terms regard the Heavy Duty Truck category, where the HDT EFs estimated in Modena are 4.28 and 5.34 g km^{-1} for petrol and diesel respectively, while the average hot EFs for the same vehicles category are 6.75 and 3.97 g km^{-1}. The variability between diesel HDT EF for the six European countries considered is also large and the maximum of these EFs is greater than the EF considered in Modena. On the other hand, diesel LDV EFs are very similar to each other and equal to 1.47 g km^{-1} for Modena and 1.58 g km^{-1} for the average EF between the six countries. By contrast, petrol LDV EFs differ of about 0.37 g km^{-1} (0.83 g km^{-1} for Modena and 0.46 g km^{-1} for the average of the other countries). Finally, Motorcycle and Passenger Cars EFs estimated in Modena agree very well with the average EFs estimated following the HBEFA methodology: 0.28 (petrol), 1.02 (diesel) and 0.05 (CNG) g km^{-1} are the PC EFs estimated in Modena, while the HBEFA respective average is 0.16, 0.94 and 0.18 g km^{-1}. Motorcycle EFs are almost the same, 0.15 g km^{-1} for Modena and 0.16 g km^{-1} for the HBEFA average.

3 Model Simulations

Following the setup described in the previous section, simulations were performed for the period between 28 October 2016 and 8 November 2016, the same period whereby the traffic measurement campaign was carried out. These days were characterized by weather condition typical for autumn in the central Po Valley (Bigi et al., 2012, Thunis et al., 2009) with a very little atmospheric circulation due to recurrent thermal inversions at low altitude, low mixing layer heights and persistent foggy and hazy events which lasted also during day time. Recurrent wind calm episodes and high-pressure conditions enhance persistence and homogenization of air masses on a regional scale: the characteristic climate conditions, along with the strong anthropic pressure in the area, lead to long-lasting high concentrations of pollutants also at remote rural sites (Bigi et al., 2017, Masiol et al., 2015, Tositti et al., 2014).

Low rainfall rate (cumulative precipitation lower than 10mm), mean wind speed lower than 2 m s^{-1} and daily average temperature from 7.4 to 13.6 °C characterized the meteorological condition in Modena during the investigated period.

WRF-Chem was performed using a 2 days spin-up period to ensure consistency with meteorological and chemical fields, as well as PMSS was executed using 6 hours of spin-up at the beginning of the simulation.

4 Model Evaluation

The statistical performance analysis considered multiple statistical indicators regardless of the model's application since each one has its advantages and disadvantages and it is not possible to identify a unique exhaustive index of quality.

The main statistical metrics employed in this study are Pearson correlation coefficient (*r*), Mean Bias (MB), Normalized Mean Bias (NMB), Root Mean Square Error (RMSE), Mean Absolute Error (MAE) and the fraction of predicted values within a factor of two of observations, also referred as Factor of two (FAC2). These statistical indicators are defined as follows, with *n* the number of model–observation pairs, *M* the modelled values (with $\bar{M} = \frac{\sum_{i=1}^{n} M_i}{n}$ the averaged modelled value) and *O* the observations (with $\bar{O} = \frac{\sum_{i=1}^{n} O_i}{n}$ the averaged observed value):

$$r = \frac{\sum_{i=1}^{n}(M_i - \bar{M})(O_i - \bar{O})}{\sqrt{\sum_{i=1}^{n}(M_i - \bar{M})^2}\sqrt{\sum_{i=1}^{n}(O_i - \bar{O})^2}}$$

$$MB = \frac{1}{n}\sum_{i=1}^{n} M_i - O_i$$

$$NMB = \frac{\sum_{i=1}^{n} M_i - O_i}{\sum_{i=1}^{n} O_i}$$

$$RMSE = \sqrt{\frac{1}{n}\sum_{i=1}^{n}(O_i - M_i)^2}$$

$$MAE = \frac{\sum_{i=1}^{n} DWD_i}{n}$$

$$where\ DWD(\text{difference of the wind direction})is\ calculated\ from:$$

$$DWD_i = \begin{cases} \min(M-O, O-M+360), & for\ M > O \\ \min(O-M, M-O+360), & for\ M < O \end{cases}$$

$$FAC2\ (fraction\ where\ 0.5 < \frac{M}{O} < 2\ )$$

In order to evaluate the performance of the models in urban environment, the Fractional Mean Bias (FB), Normalized Absolute Difference (NAD) and Normalized Mean Square Error (NMSE) were also considered. They can be defined as follow:

$$FB = 2\frac{\overline{O-M}}{\bar{O}+\bar{M}}$$

$$NAD = \frac{\overline{|O-M|}}{\bar{O}+\bar{M}}$$

$$NMSE = \frac{\overline{(O-M)^2}}{\bar{O}\cdot\bar{M}}$$

5 Results and discussion

5.1 Meteorology

2 m temperature (T2), 10 m wind speed (ws10) and 10 m wind direction (wd10) meteorological fields predicted by WRF-Chem were compared against corresponding surface observations of these variables provided by 33 stations within the d03 domain (see Table 3 and Figure 6): 18 stations (with 16 of them for T2, ws10 and wd10) belong to the RIRER (Rete idro-meteo-pluviometrica integrata) Arpae-Simc network, 11 stations (with 7 for T2, ws10 and wd 10) belong to the Archivio dati idro-nivo-meteorologici ARPA Lombardia network, 4 stations belong to the Osservatorio Meteo Idrologico della Regione Liguria (OMIRL) ARPAL network. Other two stations belonging to the Osservatorio Geofisico di Modena weather network were considered for the micro-scale wind field evaluation. All the meteorological stations mentioned before are automated and realized according to WMO (World Meteorological Organization) directive. On the other hand, NO_x concentrations at air quality stations are measured using chemiluminescence. With this method all the NO_2 contained in an air sample is converted to NO with a molybdenum converter, then the sample gas goes straight to the reaction chamber where NO (both the original NO contained in the air sample and the NO_2 converted to NO) will react with O_3 to form NO_2 and O_2 while emitting light. Finally, the measure of the emitted light will be proportional to the NO_x concentrations in the air sample.

Table 3: Observation sites. Locations are provided in Geographic coordinates (WGS84). Available parameters are: "T2" for temperature at 2 m height above the ground, "ws10" for wind speed and "wd10" for wind direction at 10 m above the ground and "NO_x" for NO_x concentrations.

Station name	Label	Network	Longitude (°)	Latitude (°)	Type	Parameters
Bologna urbana	BOL	Arpae-Simc	11.32879	44.50075	Meteorology	T2, ws10, wd10
Colorno	COL	Arpae-Simc	10.34959	44.94378	Meteorology	T2, ws10, wd10
Ferrara urbana	FER	Arpae-Simc	11.621138	44.832498	Meteorology	T2
Finale Emilia	FIN	Arpae-Simc	11.284	44.839	Meteorology	T2
Granarolo Faentino	GRA	Arpae-Simc	11.95861	44.36013	Meteorology	T2, ws10, wd10
Imola	IMO	Arpae-Simc	11.74953	44.3332	Meteorology	T2, ws10, wd10
Loiano	LOI	Arpae-Simc	11.32646	44.26093	Meteorology	T2, ws10, wd10
Malborghetto di Boara	MAL	Arpae-Simc	11.66134	44.85799	Meteorology	T2, ws10, wd10
Modena urbana	MOD	Arpae-Simc	10.91699	44.65639	Meteorology	T2, ws10, wd10
Panocchia	PAN	Arpae-Simc	10.29584	44.6837	Meteorology	T2, ws10, wd10
Parma urbana	PAR	Arpae-Simc	10.33049	44.808	Meteorology	T2, ws10, wd10
Reggio Emilia urbana	REG	Arpae-Simc	10.6337	44.69781	Meteorology	T2, ws10, wd10
Rolo	ROL	Arpae-Simc	10.874	44.88481	Meteorology	T2, ws10, wd10
S.Pietro Capofiume	SPC	Arpae-Simc	11.62264	44.65378	Meteorology	T2, ws10, wd10
San Pancrazio	SPA	Arpae-Simc	10.27245	44.80806	Meteorology	T2, ws10, wd10
Sasso Marconi	SAS	Arpae-Simc	11.24125	44.43967	Meteorology	T2, ws10, wd10
Sivizzano	SIV	Arpae-Simc	10.35704	44.6482	Meteorology	T2, ws10, wd10
Vignola	VIG	Arpae-Simc	11.00414	44.50405	Meteorology	T2, ws10, wd10
Bigarello	BIG	ARPA Lombardia	10.8874	45.18783	Meteorology	T2, ws10, wd10
Cremona	CRE	ARPA Lombardia	10.04414	45.14188	Meteorology	T2, ws10, wd10
Gambara	GAM	ARPA Lombardia	10.29949	45.24903	Meteorology	T2, ws10, wd10
Gonzaga	GON	ARPA Lombardia	10.7678	44.96381	Meteorology	T2
Mantova Lunetta	MAL	ARPA Lombardia	10.82421	45.15733	Meteorology	T2, ws10, wd10
Mantova Tridolino	MAT	ARPA Lombardia	10.86007	45.15135	Meteorology	T2, ws10, wd10
Mantova Virgilio	MAV	ARPA Lombardia	10.79293	45.11438	Meteorology	T2
Persico Dosimo	PED	ARPA Lombardia	10.1041	45.1851	Meteorology	T2
Pieve S.Giacomo	PSG	ARPA Lombardia	10.19548	45.12107	Meteorology	T2, ws10, wd10
Ponti sul Mincio	PSM	ARPA Lombardia	10.68363	45.41211	Meteorology	T2, ws10, wd10
Spinadesco	SPI	ARPA Lombardia	10.05912	45.16297	Meteorology	T2
La Spezia	LAS	ARPAL	9.82819	44.10703	Meteorology	T2, ws10, wd10
Luni	LUN	ARPAL	10.00899	44.07491	Meteorology	T2, ws10, wd10
Monte Rocchetta	MOR	ARPAL	9.93842	44.07129	Meteorology	T2, ws10, wd10
Porto Venere	POV	ARPAL	9.83594	44.052	Meteorology	T2, ws10, wd10
Badia	BAD	Arpae Emilia-Romagna	10.28937	44.65823	Air Quality	NOx
Besenzone	BES	Arpae Emilia-Romagna	10.0192	44.9895	Air Quality	NOx

Febbio	FEB	Arpae Emilia-Romagna	10.43104	44.30071	Air Quality	NOx
Gherardi	GHE	Arpae Emilia-Romagna	11.96125	44.83975	Air Quality	NOx
Ostellato	OST	Arpae Emilia-Romagna	11.94194	44.7409	Air Quality	NOx
Parco Ballirana	PAB	Arpae Emilia-Romagna	11.98236	44.52743	Air Quality	NOx
San Pietro Capofiume	SCA	Arpae Emilia-Romagna	11.62482	44.65423	Air Quality	NOx
San Rocco	SAR	Arpae Emilia-Romagna	10.66478	44.87373	Air Quality	NOx
Schivenoglia	SCH	ARPA Lombardia	11.0761	45.01688	Air Quality	NOx
Spinadesco	SPN	ARPA Lombardia	9.930599	45.15047	Air Quality	NOx
Policlinico	POL	Osservatorio Geofisico MO	10.94429	44.63580	Meteorology	ws10, wd10
Osservatorio Geofisico	OSS	Osservatorio Geofisico MO	10.92981	44.64809	Meteorology	ws10, wd10
“Parco Ferrari”	VGA	Arpae Emilia-Romagna	10.90731	44.65157	Air Quality	NOx
“via Giardini”	PFE	Arpae Emilia-Romagna	10.90572	44.63699	Air Quality	NOx

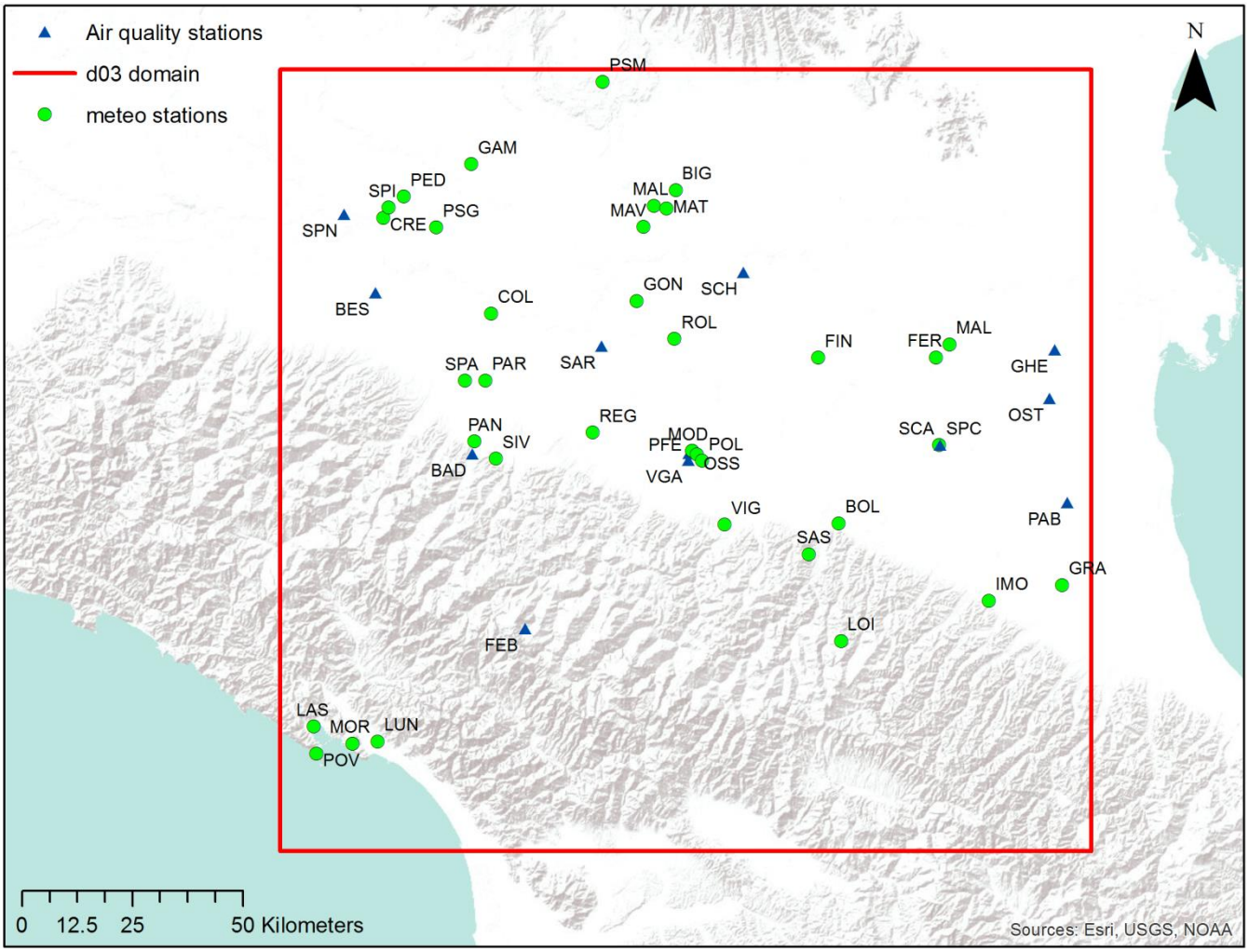

Figure 6: Map of the stations inside the WRF-Chem d03 domain. Site of the meteorological stations are reported by the green dots and site of air quality station are reported by the blue triangles.

Generally, modelled hourly 2 m temperatures reproduced by WRF-Chem at 1 km resolution (d03 domain) are consistent with observations at all the stations: *r* is between 0.68 and 0.87, except for two stations, Persico Dosimo and Bologna urbana, where the correlation is respectively very good (0.96) and not particularly high (0.59). The minimum value can be attributed to the difficulties of the model in representing urban meteorological dynamics where land use data for a large urban area may not be extremely accurate and some local phenomena can be missed. This could be the case of the Bologna city environment. By contrast, the maximum correlation observed at the Persico Dosimo station could in this case reached by a chance where hourly measurements were available only for one fourth of the investigated period. However, the good correlation between modelled 2 m temperature and observations for a large number of stations shows that the WRF-Chem model represented the observed meteorological variability quite well.

The model on average tends to be positively biased with a MB smaller than +1°C for most of the stations where only two of them exceed +2°C of MB, respectively at the Reggio Emilia urbana and Colorno stations. On the other hand, the minimum MB is -1.6°C, achieved at the Porto Venere station on to the Ligurian Sea shore. These results are in the same range as the MB that Gsella et al. (2014) found using MM5, WRF and TRAMPER meteorology models for the same area.

Figure 7 shows the statistical performance of WRF-Chem in reproducing 2 m temperature. *r* is plotted as a function of MB for the three different model resolutions: 15 km (d01), 3 km (d02) and 1km (d03). The variability of MB tends to increase by increasing the model resolution, conversely, the average *r* including all the stations is 0.78 for the d01 WRF-Chem domain, 0.80 for the d02 domain and 0.81 for the d03 domain, showing that the increase of the model resolution from 15 km to 1 km generally leads to slightly improve the performance of the model in reproducing 2 m temperature.

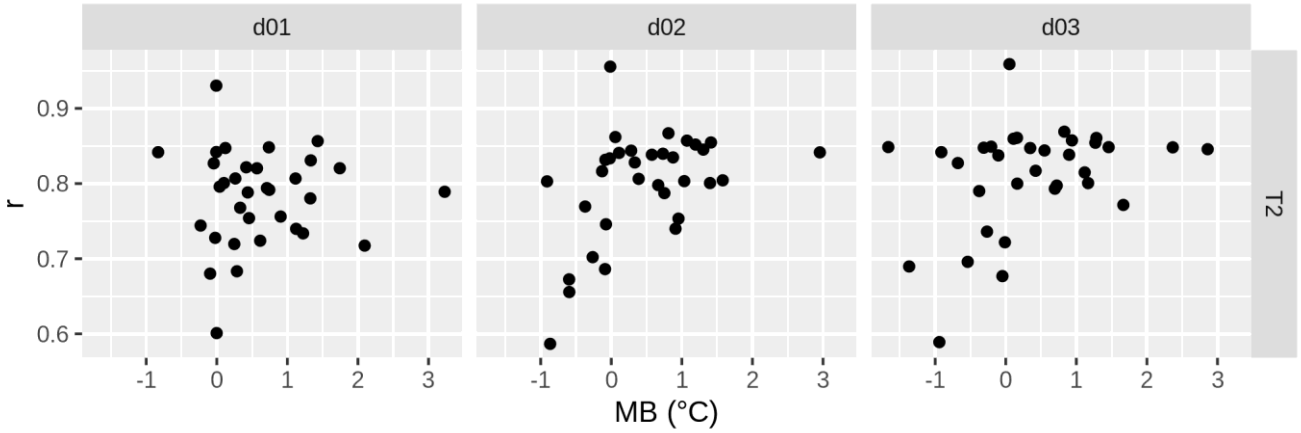

Figure 7: Pearson correlation coefficient (*r*) reported as function of the Mean Bias (MB) between modelled hourly 2 m temperature (T2) and observation at 33 measurements sites for the three WRF-Chem resolutions: 15 km (d01), 3 km (d02) and 1 km (d03).

Simulated hourly wind speed at the d03 domain generally express performance in line with similar case study in literature (Kuik et al., 2016, Mar et al., 2016, Gsella et al., 2014) since the great majority of the stations exhibits a MB between -0.5 m s^{-1} and +0.5 m s^{-1}, range suggested by Malm et al. (2009) and by European Environmental Agency (EEA) guidelines (EEA, 2011). Only the stations of Loiano and La Spezia are outside these limits with respectively a MB of -0.99 m s^{-1} and +1.43 m s^{-1}: the former is located in the Tuscan-Emilian Apennines at about 700 m above the sea level and the latter is close the Ligurian sea and then characterized by a strong influence of land-sea breeze, similarly to the temperature monitoring station of Porto Venere. The large bias found at these two stations suggests that the model might have difficulties in simulating the wind field in mountainous areas and close to the sea where complex orography and local breeze characterize the territory, however for the rest of the stations the MB values are consistent with the reference benchmarks proposed in literature.

Another statistical indicator suggested by the EEA guidelines (2011) and by Malm et al. (2009) is the Root Mean Square Error, for which the recommended benchmark for wind speed is less than 2 m s^{-1}. As for the MB, RMSE of modelled wind speed values are below 2 m s^{-1} at all stations besides Loiano and La Spezia, where RMSE are 3.76 m s^{-1} and 2.14 m s^{-1},

respectively. Nonetheless, modelled wind speed at the vast majority of the stations is in line with the benchmark for a mesoscale meteorological reconstruction.

In Figure 8 the performance of WRF-Chem in reproducing wind speed for the three different resolutions is shown: RMSE is plotted as a function of the MB. As the resolution is increased, the model tends to show lower MB in absolute terms. Similarly, the RMSE generally tends to moderately decrease as well with increasing resolution. It is therefore possible to conclude that in increasing model resolution from 15 km to 1 km there is a slight improvement of performance also for wind speed reconstruction.

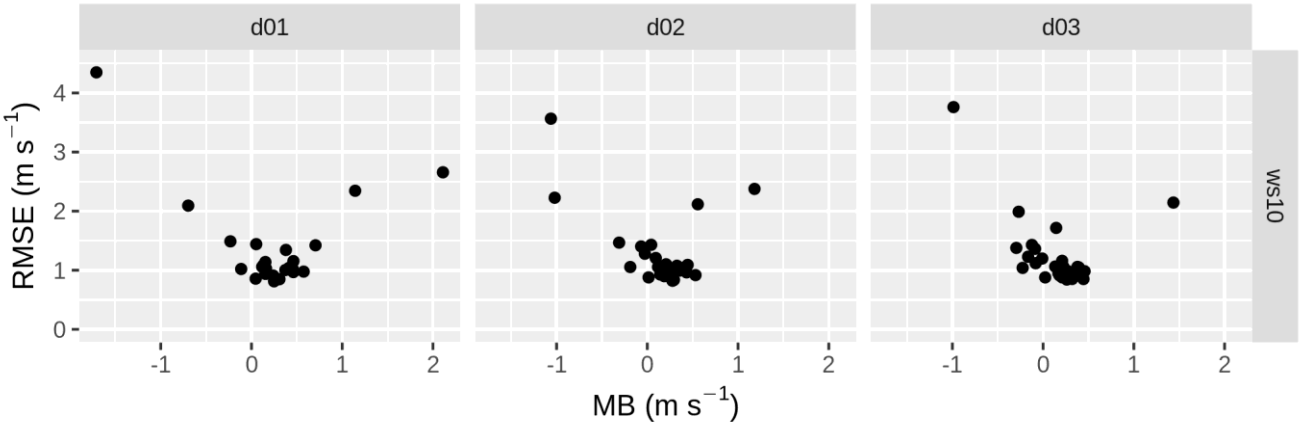

Figure 8: Root Mean Square Error (RMSE) reported as function of the Mean Bias (MB) between modelled hourly 10 m wind speed (ws10) and observation at 27 measurements sites for the three WRF-Chem resolutions: 15 km (d01), 3 km (d02) and 1 km (d03).

Despite the WRF-Chem performance in reproducing observed wind speed were satisfactory, wind direction at the same locations were in general poorly reproduced by the model in all the three domains. The MAE statistical indicator, modified as indicated in section 4 to meet the special requirement for circular data, was used to quantify the model capability to capture measured wind direction. In Figure 9 MAE is plotted in function of RMSE, where nevertheless this later one ignores the particularities of circular data, it has been applied in several previous studies for wind direction evaluation. WRF-Chem captured particularly well wind direction at Loiano station where RMSE is around 85° for all the three domains and MAE is 33° for domain d01 and 38° for domain d02 and d03. By contrast wind direction at Parma urbana and Reggio Emilia urbana stations the model expressed the maximum MAE with values respectively equal to 80° (domain d01) and 82° (for both d02 and d03 domains), with RMSE about 140° at Parma urbana station for all the three domains and equal to 127° (domain d01) and 137° (domain d02 and d03) at Reggio urbana.

Although the model performances in reproducing the wind directions are not outstanding, they are in line with other case studies within the Po Valley, where MAE was between 42° and 93° (Gsella et al., 2014, de Meij et al., 2009) and RMSE was between 127° and 148° (Gsella et al., 2014), confirming the difficulties in modelling the wind fields in this area characterized during winter and fall time by stagnant conditions and low wind speed.

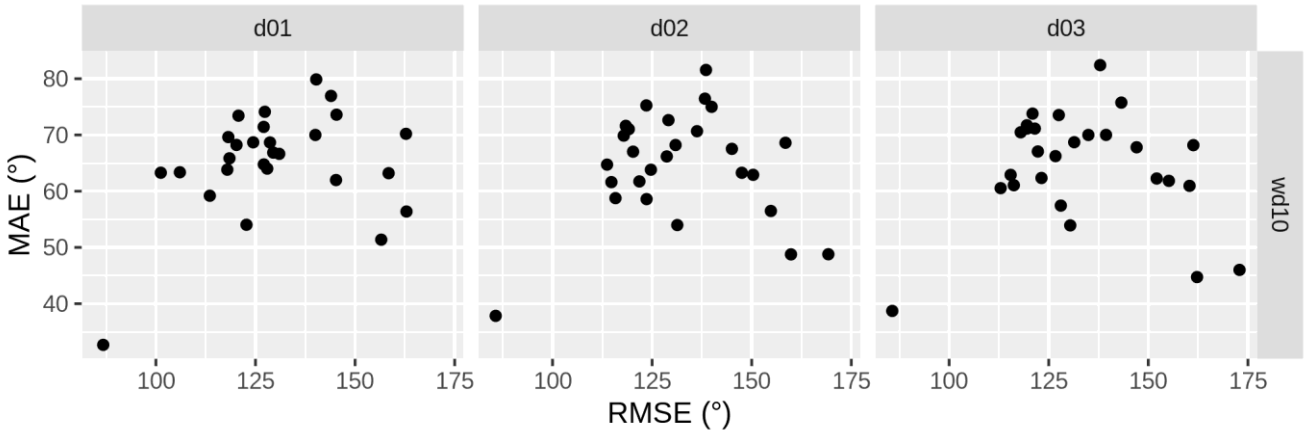

Figure 9: Mean Absolute Error (MAE) reported as function of the Root Mean Square Error (RMSE) between modelled hourly 10 m wind direction (wd10) and observation at 27 measurements sites for the three WRF-Chem resolutions: 15 km (d01), 3 km (d02) and 1 km (d03).

5.2 WRF-Chem nitrogen oxides

Since the role of WRF-Chem in this study was to estimate NO_x ($NO + NO_2$) concentrations due to emissions on the regional scale that may affect the background air quality in Modena, modelled hourly NO_x concentrations were compared with observations at 10 rural background sites (8 of them from the Arpae Emilia-Romagna network and 2 of them from Arpa Lombardia network, see Table 3 and Figure 6) within the d03 WRF-Chem domain.

Modelled NO_x concentration at 1 km resolution is biased negatively for 8 stations with a minimum MB equal to -18.1 µg m^{-3} (-62% of NMB) and biased positively for 2 stations with a maximum MB of +7.8 µg m^{-3}(+30% of NMB). In addition, for each reference station, the fraction of predicted values within a factor of two of observations was computed, also referred as FAC2. The corresponding average value over all stations is 56% (minimum 30% at the station of Ostellato and maximum 76% at the stations of Schivenoglia), in accordance with the reference value suggested by Chang and Hanna (2004), greater or equal to 50%.

In order to test which level of model spatial resolution gives better results, observed NO_x concentrations were compared with modelled concentrations at 15 km (d01) and 3 km (d02) resolutions in terms of FAC2 and NMB (Figure 10). The model at 15 km resolution presents on average the highest FAC2 with respect other configuration, 62% (maximum equal to 82% at the stations of Schivenoglia and minimum equal to 39% at the station of Ostellato), conversely the NMB presents its higher variability, from -58.9% to 122.2% (respectively -17.5 µg m^{-3} and +5.7 µg m^{-3} of MB).

Among the other configurations, WRF-Chem at 3 km resolution shows better performance with an averaged FAC2 between all the stations equal to 61% (79% of maximum at Langhirano station and 37% of minimum at the station of Ostellato) and the smallest variability between all the stations in terms of NMB, from -56.6% to 28.7% (respectively -16.8 µg m^{-3} and +1.3 µg m^{-3} of MB).

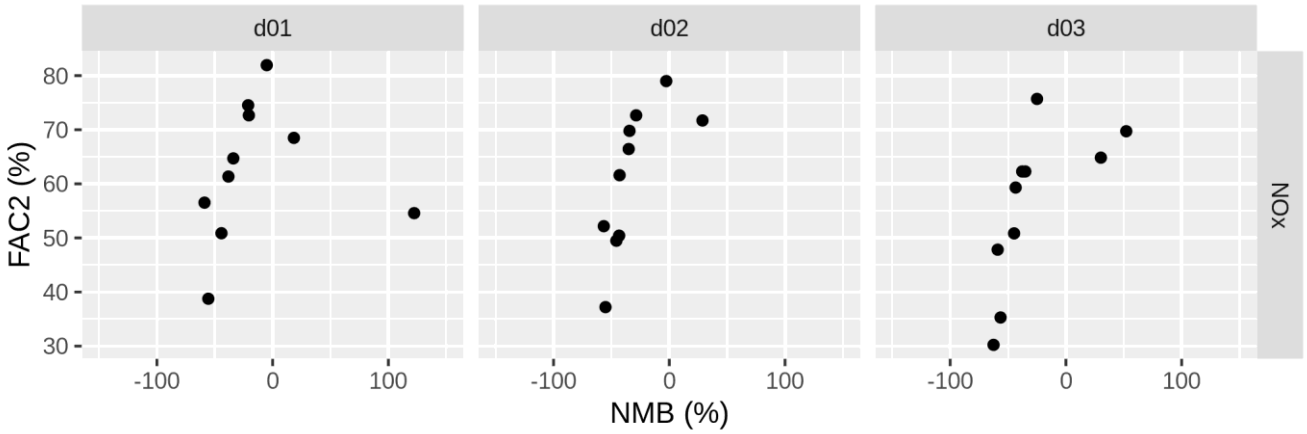

Figure 10: Factor of two (FAC2) reported in function of the Normalized Mean Bias (MB) between modelled hourly NO_x concentrations and observation at 10 rural background sites for the three WRF-Chem resolutions: 15 km (d01), 3 km (d02) and 1 km (d03).

The comparison showed that generally the WRF-Chem model with a horizontal resolution of 3 km is better suited to reproduce NO_x concentrations at rural background sites considering an emission inventory of 14 km x 7 km resolution. Increasing resolution to 1 km, the model tends to decrease the number of predicted concentrations within a factor of two of observations, despite the variability of the NMB being approximately the same as the configuration at 3 km. It is also worth remarking that nonetheless the modelled NO_x concentrations are on average in agreement with the values suggested by Chang and Hanna (2004) for model performance evaluation in terms of NMB and FAC2, not all considered stations satisfy these statistical indicators, this might mean that a more detailed emissions estimation such as an improved emissions distribution in the area should be implemented to achieve better results.

5.3 WRF-Chem combined with PMSS

5.3.1 Micro-scale wind fields

High resolution winds in the urban area of Modena were estimated by the means of Micro-SWIFT (the 3D mass-consistent diagnostic model that composes PMSS), initialised with the meteorological fields reproduced by WRF-Chem at hourly time step. Simulated winds reproduced by Micro-SWIFT were compared with observation at three different meteorological sites located within the urban center of the city. These stations are respectively placed on top to the Geophysical Observatory tower, at 42 m height above the ground and placed in the historical part of the city (referred as OSS), above the public hospital to the Est of the historical city center at about 20 m height (referred as POL), and on top to the municipality building at 40 m height, to the West of the historical city center (MOD station), the latter used also to validate the WRF-Chem meteorology. Figure 4 depicts the position of these three stations.

The time series reported in Figure 11 show the comparison between modelled and measured hourly wind speed for the three urban meteorological sites. Notwithstanding a few remarkable overestimations on November 3, 5 and 7, mostly visible at the OSS and MOD stations, modelled data reproduced observed trend quite well for all the three locations. MOD and OSS modelled time series show also a very similar behaviour (with a general less pronounced overestimation for MOD on November 3, 5 and 7) due to the location of the sensor, both above 40 m and thus characterized by the same meteorological input and not affected by the presence of buildings.

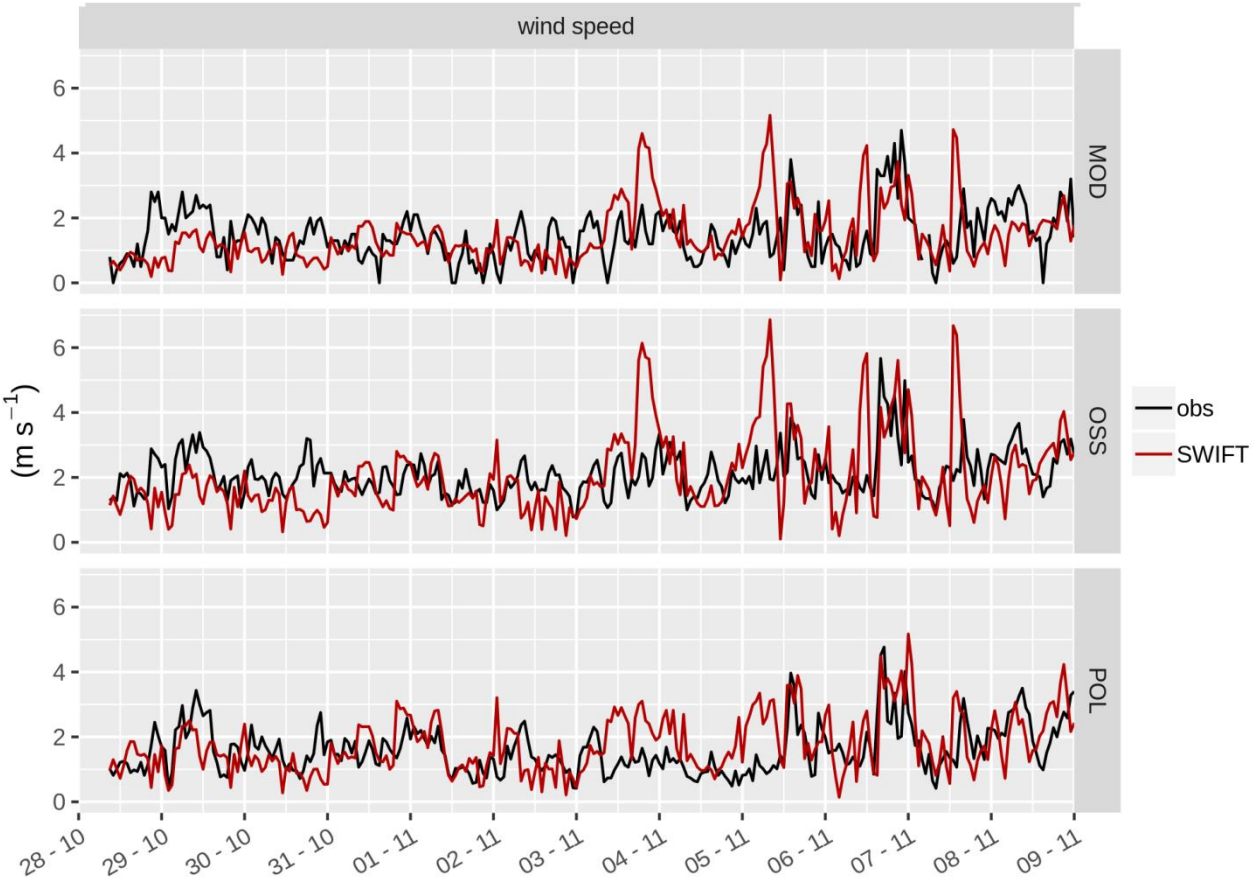

Figure 11: Hourly observed wind speed at MOD (on top), at OSS (in the middle) and at POL (on bottom) meteorological site along with hourly simulated wind speed by Micro-SWIFT, from October 28 to November 8, 2016.

The satisfactory performances showed by the time series regarding wind speed are also confirmed by the statistical metrics. The MB is less than 0.2 m s^{-1} for all the three stations and the RMSE is between 0.93 and 1.24 m s^{-1}. FB and FAC2 are also in line with the values found during the validation of the PMSS modelling suite in urban environment (Oldrini et al., 2019). Table 4 summarizes computed metrics.

Table 4: Statistics of hourly wind speed computed for the period between October 28 and November 8 at three urban meteorological stations.

Station	FB	MB	NMB	RMSE	FAC2
MOD	0.003	-0.005	-0.3%	1.05	0.67
OSS	0.03	-0.05	2%	1.24	0.76
POL	-0.10	0.17	11%	0.93	0.76

In Figure 12 hourly simulated wind directions are compared with hourly observed wind for the same three locations. As for regional wind field evaluation, wind directions were poorly reproduced by Micro-SWIFT, respectively with MAE equal to 125° for the MOD station, 124° for OSS and 114° for POL. By contrast the performance of Micro-SWIFT evaluated in terms of FB and NMSE are similar to the results obtained in urban environment by Oldrini et al. (2019) using the same model: for MOD site the FB and NMSE are respectively equal to 0.21 and 0.76, FB is 0.23 for both OSS and POL locations and NMSE is 0.80 and 0.70 at OSS and POL stations.

This poor behaviour in wind direction reconstruction can be partly attributed to the input data used by Micro-SWIFT, which reflects the bias given by the regional forecast model in wind direction estimation. This is mainly due to the difficulty of the meteorological models in reproducing wind fields during the situations with very little atmospheric circulation (stagnant condition) and low wind speed, as occur red in this case study (Gsella et al., 2014, de Meij et al., 2009).

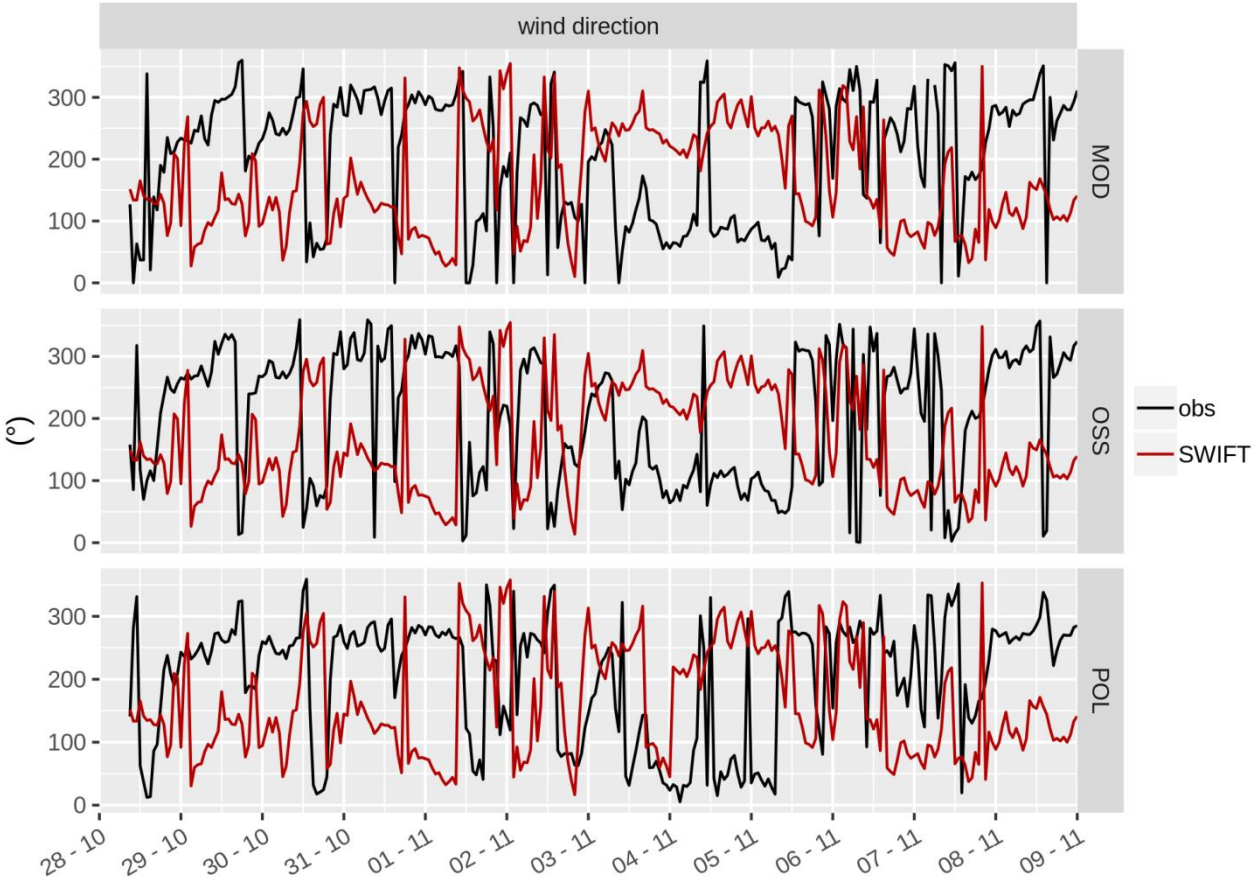

Figure 12: Hourly observed wind direction at MOD (on top), at OSS (in the middle) and at POL (on bottom) meteorological sites along with hourly simulated wind direction by Micro-SWIFT, from October 28 to November 8, 2016.

5.3.2 Micro-scale NO_x concentrations

NO_x background concentrations estimated with WRF-Chem in the urban area of Modena were added to the NO_x simulated concentrations reproduced with PMSS modelling system performed considering exclusively road traffic emissions. Modelled concentrations were compared with observations at two urban stations: the first one at a traffic site, located in the proximity of a busy street close to the urban ring road, named "via Giardini", and the second one at background site, within a public park to the West of the historical city centre, named "parco Ferrari" (Figure 4).

In Figure 13, the hourly NO_x concentrations predicted by PMSS in combination with WRF-Chem at 3 km and 1 km resolutions (labelled as "d02+ PMSS" and as "d03+ PMSS") are compared through scatter plots for both urban traffic and background stations. In this figure, the solid line represents perfect agreement with observations and within the dashed lines modelling results and observations agree with a factor of two.

Most of the modelled data are within a factor of two of observations, especially for the urban traffic site in both WRF-Chem configurations, whereas for the urban background station an under estimation is more noticeable. It is also worth noting that the results of PMSS combined with WRF-Chem at 3 km and at 1 km resolution depict similar behaviour and relative scatter plots are very comparable to each other, with a slightly less pronounced underestimation for WRF-Chem at 3 km resolution.

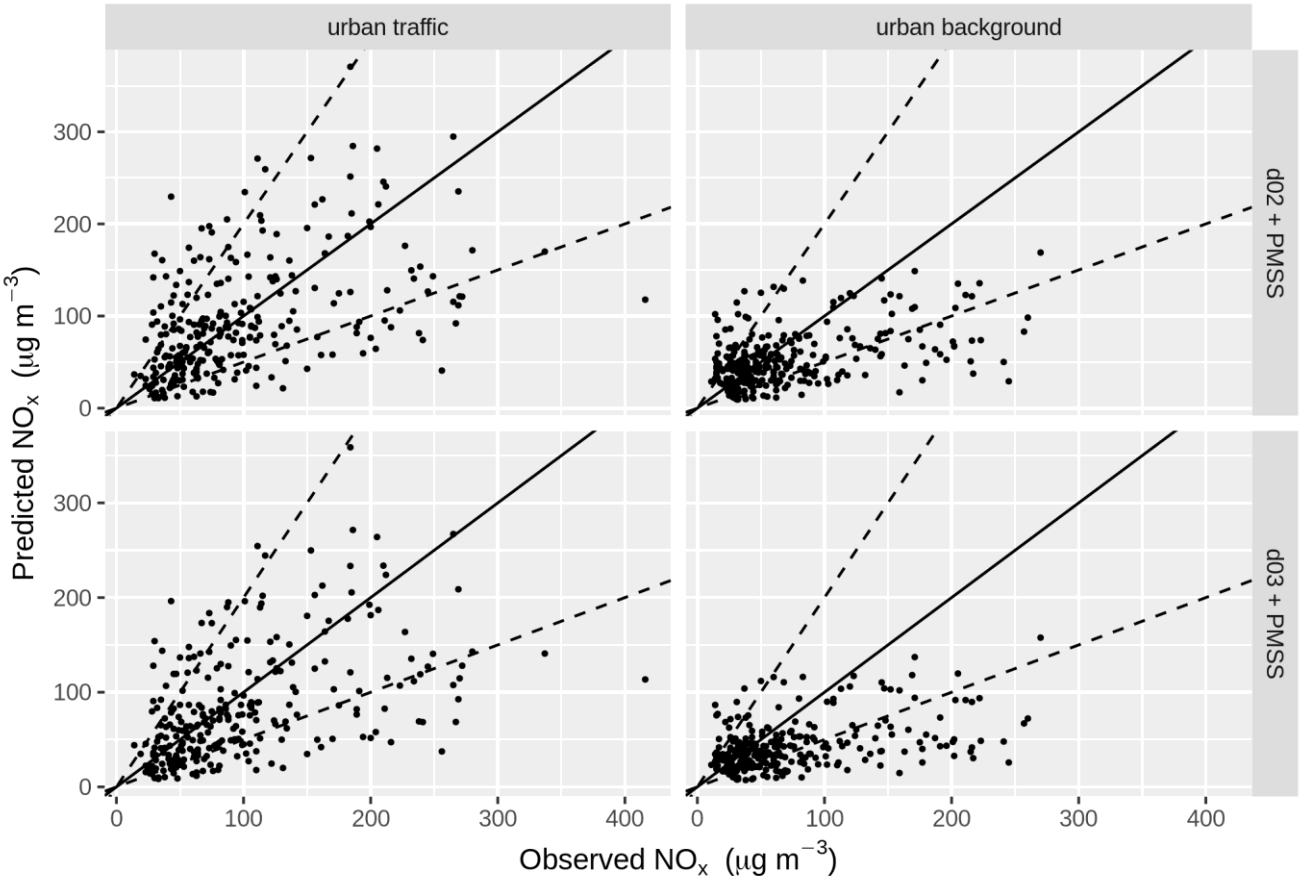

Figure 13: Scatter plots of predicted NO_x concentrations at urban traffic ("via Giardini") and urban background ("parco Ferrari") stations for different models configurations: PMSS combined with WRF-Chem at 3 km resolution (labelled as "d02+PMSS") and PMSS combined with WRF-Chem at 1 km resolution (labelled as "d03+PMSS").

Modelled hourly NO_x concentrations are biased negatively in both urban stations: at the "via Giardini" traffic site the MB of simulated NO_x by PMSS and WRF-Chem at 1 km resolution is -15 µg m^{-3}, which corresponds to -15% of NMB, for the same model configuration the MB at the "parco Ferrari" background site is -30 µg m^{-3} (-41% NMB). Modelled hourly

concentrations correlate reasonably well with observations in both sites, with *r* equal to 0.48 at the traffic station and 0.43 at the background station.

The performance of the models generally increases when hourly NO_x concentrations reproduced by PMSS are combined with the results of WRF-Chem at 3 km resolution, the MB at the "via Giardini" traffic station is -4 µg m^{-3} (-4% NMB) and -18 µg m^{-3} (-25% NMB) at the "parco Ferrari" measurement station.

Despite an improvement in term of MB with WRF-Chem at 3 km, its combination with PMSS doesn't particularly affect the *r* between modelled and observed concentrations (0.47 at "via Giardini" traffic station and 0.44 at "parco Ferrari" background site).

A quantitative estimation of the agreement between simulated and observed concentrations was also assessed following the statistical metrics proposed by Hanna and Chang (2012) for urban dispersion model evaluation. FB, NMSE, FAC2 and NAD were computed for both the urban stations located in Modena and for both the combination of WRF-Chem (3 km and 1 km resolution) with PMSS. Table 5 summarizes all the computed statistics.

Following Hanna and Chang (2012) the reference acceptance criteria for the aforementioned metrics in urban dispersion model evaluation are as follows:

- |FB| < 0.67, i.e. the relative mean bias is less than a factor of ~2
- NMSE < 6, i.e. the random scatter is less than 2.4 times the mean
- FAC2 > 0.30, i.e. the fraction of predicted concentrations within a factor of two of observed concentrations exceeds 0.30
- NAD < 0.50, i.e. the fractional area for errors is less than 0.5

Table 5: Statistics of hourly NO_x concentrations computed for the period between October 28 and November 8, considering two different model configurations.

Configuration	Station	FB	NMSE	FAC2	NAD
PMSS + d02	urban traffic	0.04	0.48	0.72	0.24
	urban background	0.29	0.75	0.62	0.29
PMSS + d03	urban traffic	0.16	0.54	0.68	0.26
	urban background	0.52	1.15	0.59	0.35

The statistical analysis shows that PMSS combined with WRF-Chem at both d02 and d03 domains fulfill the acceptance criteria defined by Hanna and Chang (2012). Regarding the FB, the results are always less than the threshold of 0.67, in particular at urban traffic site the outcomes of this metric are particularly good with values equal to 0.04 (PMSS + d02) and 0.16 (PMSS + d03). At urban background station the results are larger than the previous one (0.29 for PMSS + d02 and 0.52 for PMSS + d03) indicating that the models tend to underestimate more the mean concentrations but nevertheless in well

agreement with the reference benchmark. As far as the NMSE is concerned, the models show their best performances with scores largely lower than the acceptance benchmark (6), with a maximum value of 1.15 at urban background station for PMSS + d03 (minimum value at traffic station for PMSS + d03 equal to 0.48), meaning that predicted values very rarely differ strongly from observations.

Regarding the FAC2 and the NAD there is a significant agreement between model results and relative acceptance criteria at both urban stations and for both model configurations. Minimum and maximum FAC2 are equal to 0.59 and 0.72 achieved respectively at the urban background station for PMSS + d03 and at urban traffic station for PMSS + d02 (the lower limit proposed by Hanna and Chang is 0.30). For the same locations and model configuration the maximum and the minimum NAD are 0.35 and 0.24 respectively (upper limit proposed by Hanna and Chang is 0.50).

The statistical analysis, despite supporting a moderately better behaviour when the resolution of WRF-Chem is 3 km, also shows that the metrics of modelled NO_x concentrations are comparable between the two WRF-Chem resolutions (1 km and 3 km), without a clear difference of one of the two.

Time series analysis (Figure 14) shows that modelled NO_x concentrations agree quite well with observations. In particular for the first five days of simulations (considering the combination with WRF-Chem at 3 km resolution as a reference), between October 28 and November 1st observations are reproduced well and daily peaks are modelled with quite good accuracy, especially for urban traffic station where the MB between October 28 and November 1 is +7µg m^{-3} and NMB is about 1% (at the background station the MB is -14 µg m^{-3} and NMB is -1%).

By contrast, between November 1 and 2 observed NO_x concentrations tend to be overestimated since the WRF-Chem contribution during the central hour of days exceeds observed NO_x concentrations. This situation is particularly evident at the "parco Ferrari" station. Furthermore, between November 2 and 3, PMSS failed to capture the diurnal cycle in observed concentrations: on November 2 in the central hours of the day observations are largely overestimated with an increasing trend up to the afternoon peak. A possible explanation to this episode can be addressed to an underestimation of the PBL height during the central hours of the day, where its modelled value doesn't exceed 190 m (average daily maximum during the whole simulation is 600 m) and during only 6 hours the modelled PBL height is greater than 100 m.

On the other hand, on November 3, when observed concentrations reach values over 200 µg m^{-3}, the models underestimate the observed values. Between November 4 and November 6 observed NO_x concentrations were lower than in the previous days (hourly maximum always lower than 200 µg m^{-3}) mostly due to the rainfall which occurred on November 5 (8 mm) and 6 (1 mm), where the combination of the two models was able to reproduce the hourly pattern well, with a slight overestimation at the traffic station.

On November 7 and 8 extremely high peaks occurred with values that exceeded 400 µg m^{-3} at urban traffic station and 250 µg m^{-3} at urban background station. Despite an underestimation of absolute observed NO_x concentrations experienced on these two days, the shape of the diurnal cycle was captured quite well by the models.

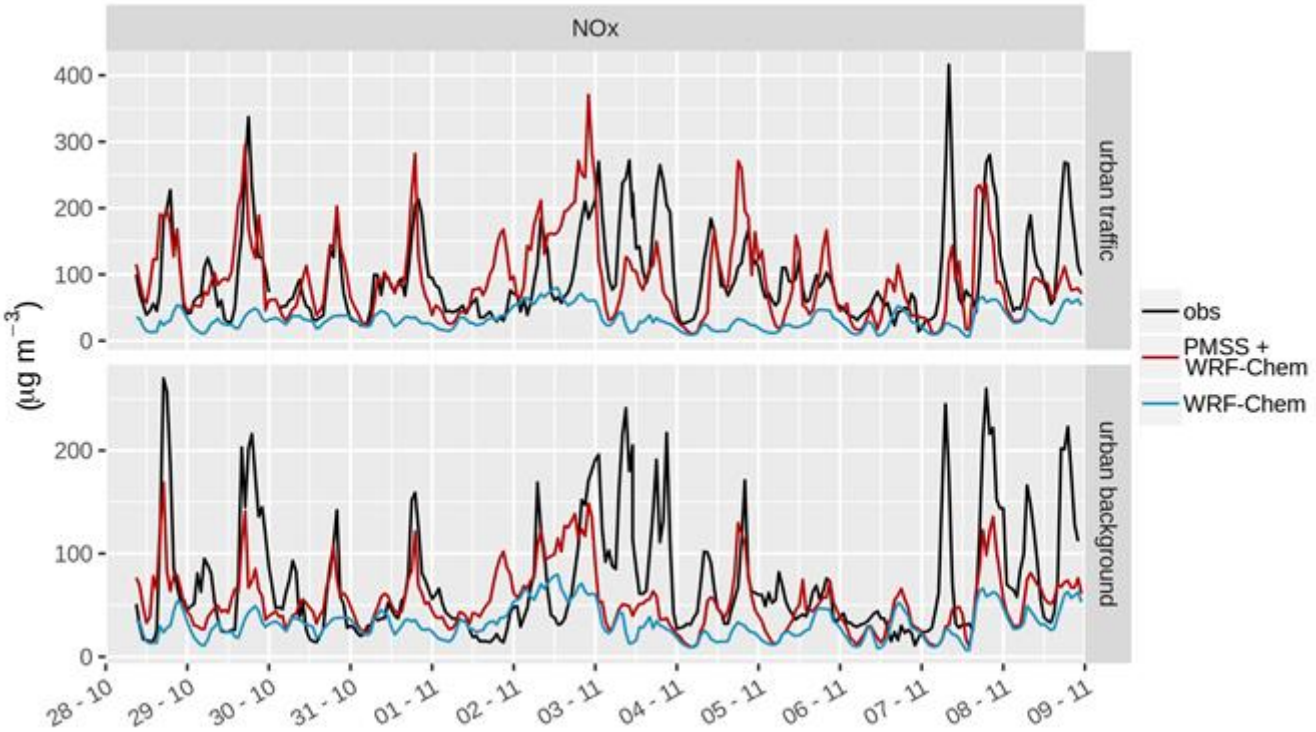

Figure 14: Hourly observed concentrations of NO_x at urban traffic (on top) and urban background (on bottom) measurements stations along with hourly simulated concentrations by WRF-Chem at 3 km resolution and PMSS combined with WRF-Chem at the same resolution, from October 28 to November 8, 2016. Please note the difference in the scale on the y-axis in each panel.

Finally, in order to study which part of day primarily affected the general underestimation of the models and to investigate the WRF-Chem contribution to the total NO_x concentrations during the day, the variation of observed and predicted NO_x concentrations by hour of the day was assessed. The comparison of mean observed NO_x daily cycle shows very similar behaviour between the "via Giardini" and "parco Ferrari" stations (Figure 16): two main peaks occur on average during the day, one between 08:00 and 09:00 a.m. (equal to 150 µg m^{-3} at traffic site and 105 µg m^{-3} at background site) and the second, on average greater of about 20-30 µg m^{-3} than the former, around 07:00 p.m. (about 170 µg m^{-3} at traffic site and 140 µg m^{-3} at background site). At "parco Ferrari" station another peak occurs in the early morning (around 01:00 a.m.) less pronounced than the other two, with a mean concentration of about 70 µg m^{-3}.

For the purpose of further investigate the modelled concentrations, in Figure 15 is shown the diurnal cycle of traffic emissions used for WRF-Chem and the average diurnal cycle used for PMSS in working and non-working days. There is a large correspondence between the traffic temporal cycle of WRF-Chem and PMSS in working days. For the former, the

afternoon peak (which occurs at 06.00 p.m.) is a little more pronounced than the morning maximum (08:00 and 09:00 a.m.), while for PMSS is the opposite. During non-working days WRF-chem presents the same hourly behaviour of for working days but absolute values are quite decreased. By contrast, as far PMSS is concerned, the morning peak is at 10:00 a.m. and the afternoon maximum is at 07:00 p.m., both delayed by one hour compared to WRF-Chem.

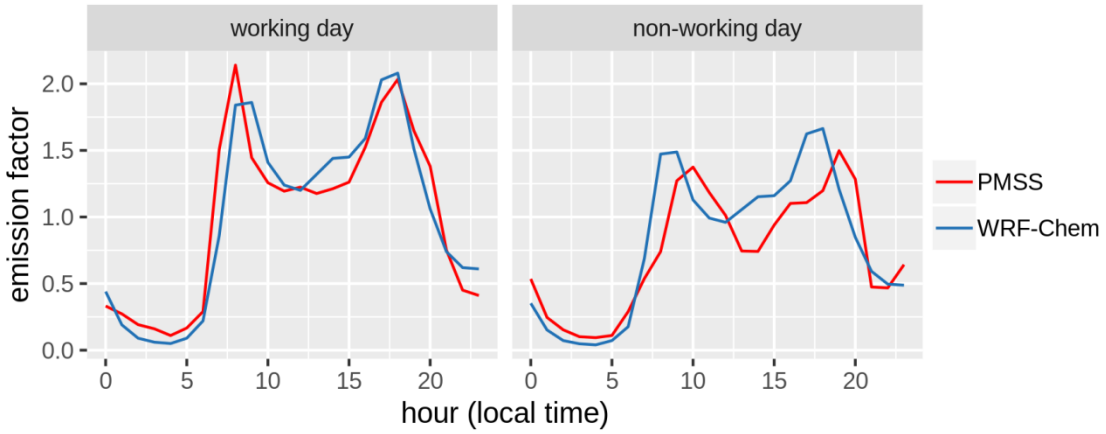

Figure 15: Overview of the diurnal cycle of the traffic emission factor for WRF-Chem (light blue) and the average diurnal cycle for PMSS (red) for working and non-working days.

Modelled daily NO_x concentrations present a good agreement with observed daily cycle for traffic station: the first peak of the day on average tending to be underestimated and despite the second peak is anticipated of about two hours, its magnitude is captured very well, especially when the WRF-Chem model is used at 3 km resolution. This confirms the advantages obtained using a detailed traffic modulation recorded on a street in the proximity of the traffic station.

On the other hand, at urban background site, the modelled daily pattern is acceptable, but absolute concentrations are generally underestimated in particular in the morning peak. This behaviour might be explained looking at the PBL height simulated by WRF-Chem and used to drive the micro-scale dispersion (Figure 16): during the night the boundary layer is stable due to surface longwave cooling and a shallow temperature inversion strong characterizing the area with a mean PBL height during night time hours for the whole simulation around 100 m. After dawn, surface heating builds up a shallow mixed layer, which deepens during the central hours of the day inducing a rising of the PBL height, on average up to 600 m. During this situation, at the background site, where the traffic emissions are less pronounced compared to the traffic site, modelled NO_x concentrations tend to be limited by the mixing phenomenon that occurs from around 07:30 a.m. onwards, causing a strong underestimation of the morning observed peak.

In the late afternoon (between 04:00 and 05:00 p.m.), the solar heating is no longer sufficient to maintain an upward surface buoyancy flux and the boundary layer becomes restricted to a shallow layer, around 100 m deep, as in the night. Under this condition NO_x concentrations increase, generating the second daily peak more pronounced than the first one and anticipated

of about two hours. A more detailed description of the PBL evolution during the day, through for example ceilometer observation, could help to improve the concentration estimation.

At urban traffic site the mechanism seems to be the same but large traffic emissions affected less the underestimation during the morning peak.

The NO_x underestimation could also be associated to the aged traffic fluxes estimated by the PTV VISUM model, which simulation reference year is 2010 and then affected by economic recession whereby all western countries have fallen since 2007. The economic crisis caused a slower growth of gross national product and an increase in unemployment which, among the other consequences, led to a reduction in traffic fluxes in the European business centres. For these reasons traffic fluxes estimated by PTV VISUM in the city of Modena may be affected by an underestimation with respect the real traffic occurred during the simulated period.

It is also worth noting that the PTV VISUM simulation doesn't include traffic fluxes of urban public transport, therefore the vast majority of urban buses emissions are not taken into account in the simulation. Due to the presence of schools nearby the "via Giardini" monitoring station, the morning rush hours (especially between 08:00 and 09:00 a.m.) are characterized by an intense flow of public buses and the consequent omission of public transport emissions can influence and contribute to the morning NO_x underestimation.

In addition, traffic fluxes in secondary streets seem to be modelled worse than busier roads and at the urban background station the NO_x underestimation can also be attributed to a rough estimation of NO_x sources around the area where traffic emissions are modulated according the measurement data collected at "via Giardini" street. Moreover, other NO_x emissions sources are simulated by the WRF-Chem model through the use of the TNO-MACC inventory which level of detail is about 7 km and thus not as exhaustive as the traffic emissions, and these other NO_x sources are expected to have larger influence at urban background than at urban traffic sites. Besides this, looking at the NO_x concentrations daily cycle, the contribution of WRF-Chem to the total simulated concentrations seems to be modest compared to direct effect of traffic emissions. In particular, when the resolution of WRF-Chem is 1 km, its share doesn't present a strong hourly trend but it is rather flat, with an average contribution during each hour of simulation in the order of 20 $\mu g\ m^{-3}$, at both traffic and background sites. On the other hand, when the resolution of WRF-Chem is 3 km, its rate to the total concentrations is greater than the one a 1 km resolution (average hourly contribution about 30 $\mu g\ m^{-3}$), with an hourly trend more marked during the two daily peaks. This difference in contribution estimate could be explained considering the position of the WRF-Chem computational cells. In the case of 1 km resolution the computational cells over "parco Ferrari" and "via Giardini" stations, even if they present very similar concentrations, are different and located both inside the PMSS domain. Conversely, for d02, both the stations are within the same computational cell and the cell itself is no longer entirely contained in the PMSS domain but it extends to the West, beyond the PMSS borders. This latter configuration leads to account within the PMSS domain part of the TNO traffic emissions occurring outside the Modena urban area, originally excluded from the PMSS computation, causing a homogenization and an increasing in NO_x concentrations over the entire WRF-Chem cell. The final outcome is that the

contribution of WRF-Chem using d02 to the urban concentrations is larger and also the daily trend during the two daily peaks appears more pronounced.

More accurate traffic modulation across the city and a finer spatial resolution of non-traffic related exhaust emissions, as well as a more accurate description of the planetary boundary layer height during the day, would better fit the 1km grid of WRF-Chem used in d03 and can certainly contribute to achieve better results also at urban background station.

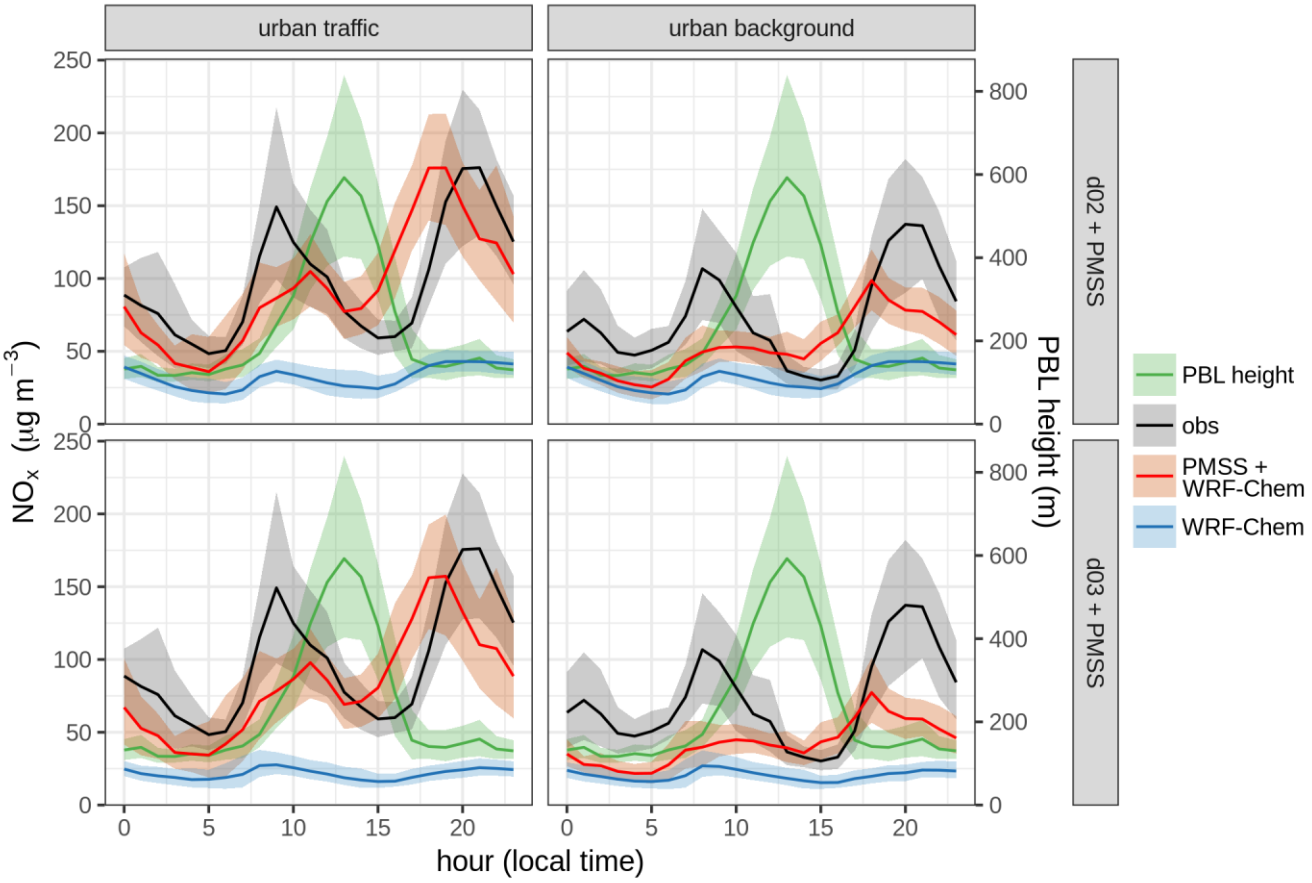

Figure 16: Mean daily cycle of observed NO_x concentrations (black), modelled by the combination of WRF-Chem and PMSS model (red) and the only contribution of WRF-Chem (light blue), by station type (traffic or background) and by WRF-Chem resolution (3 km or 1 km). Green lines show the mean daily cycle of planetary boundary layer height modelled by WRF-Chem and used in the micro-scale dispersion. Solid lines represent the daily mean cycle, meanwhile shaded area show the variability between 25th and 75th percentiles.

6 Summary and conclusions

In this study the authors evaluated a hybrid modelling system consisting of the chemical transport model WRF-Chem and the Parallel Micro SWIFT SPRAY (PMSS) modelling system for the urban area of Modena with the aim of providing NO_x

concentration maps at building-resolving scale and at hourly temporal resolution, suitable to resolve the variability of emissions and atmospheric state. The WRF-Chem model was applied over three nested domains with an increasing resolution from 15 km to 1 km passing by 3 km, in order to simulate the emissions, transport and chemical transformations at the regional scale by accounting also at the same time for meteorological phenomena at the synoptic scale. Driven by these meteorological fields, the PMSS modelling suite was run over a domain of 6 km x 6 km with 4 m grid step size, to reconstruct micro-scale wind streams inside the urban area of Modena and then to simulate the dispersion of NO_x, coming from traffic emissions, by accounting for the presence of buildings.

The 2 m temperature and 10 m wind speed were captured well by the WRF-Chem model with statistical metrics in line with benchmark values suggested by the guidelines of the European Environmental Agency for meteorological mesoscale reconstruction, and with similar case studies related to the same area. Only few exceptions were observed at particular locations such as in mountainous area or close to the Ligurian sea, where complex orography and the local sea breeze strongly influenced the model bias in reproducing the meteorology. Despite, 10 m wind direction was poorly reproduced by WRF-Chem, its performance in term MAE and RMSE was in line with other cases studies focusing on the PO Valley, suffering both from the models difficulties in reproducing wind field during the situations with very little atmospheric circulation and low wind speed. Moreover, increasing WRF-Chem resolution from 15 km to 1 km resolution generally tended to slightly improve the model performance in reproducing 2 m temperature and 10 m wind speed.

NO_x concentrations reproduced in the Po Valley area by WRF-Chem were on average simulated reasonably well, but generally underestimated in almost all the rural background monitoring stations. The comparison with observations showed also that with an emissions inventory of 7 km horizontal resolution, the 1 km model resolution does not generally improve the results and the model configuration at 3 km resolution expressed the best performance in modelling NO_x concentrations.

Simulated and observed NO_x hourly concentrations in the urban area of Modena exhibit a large agreement, in particular for urban traffic site ("via Giardini" measurement station), where detailed traffic emissions estimation (real traffic modulation combined with a bottom-up approach) proved to be very successful in reproducing the observed NO_x pattern, confirming that reasonable time modulation for traffic emissions are among the main parameters to trim for urban atmospheric dispersion. Despite the morning rush-hour peak (between 08:00 a.m. and 09:00 a.m.) tending to be generally underestimated, the magnitude of the afternoon peak around 07:00 p.m. was well captured by PMSS with an anticipation of about two hours. At the urban background station, notwithstanding a general underestimation of the observed concentrations (more pronounced than at the urban traffic site), the analysis of hourly daily modelled concentrations shows that PMSS combined with WRF-Chem provided a daily pattern in line with observations.

These features highlight the strength of this modelling chain in representing urban air quality, in particular at traffic sites, whose concentration levels make them the most critical area of the city; characteristics that chemical transport models alone cannot express, due to the coarser resolution to which they operate and to their inability to reproduce street canyons and urban structures.

Despite the inclusion of external emission sources for computational cells at PMSS boundaries, WRF-Chem at 3 km resolution generally presented slightly better results than the 1 km resolution, demonstrating that the contribution of background sources to urban pollution levels were generally underestimated and a better quantification of the emissions also in the surrounding area of Modena could improve the final result. The background underestimation may depend also on WRF–Chem perfectible effectiveness in reproducing the effects of the air mass homogenization on a regional scale that characterizes the climate conditions in central Po Valley.

The statistical analysis showed finally that PMSS combined with WRF-Chem at both the resolutions (3 km and 1 km) and both the urban measurement stations fulfil the acceptance criteria proposed by Hanna and Chang (2012) for urban dispersion model evaluation. These outcomes confirmed and proved how this tool composed of two complex modelling systems (WRF-Chem and PMSS) can be employed to support environmental policies, epidemiological studies and urban mobility planning. Based on the performances expressed by modelled concentrations with respect observations, a further application of this tool will concern the prediction of the air quality in Modena at building resolving scale based on meteorological and background concentrations forecast provided by WRF-Chem and on local sources contribution estimated with the PMSS modelling suite. Further work should focus also on other key species such as NO_2 and particulate matter (PM_{10}) and on integrating other in situ observations to better characterize the emissions and the evolution of the PBL height during the day in the urban area of Modena. For example, time-resolved and spatially-resolved CNG (compressed natural gas) consumption data can be used to estimate domestic heating emissions, and also, traffic counts recorded by induction loops spires located in the main cross-roads intersections could be exploited to better describe traffic emissions on the entire road network. As well as, urban ceilometer observation would be necessary to correctly investigate the evolution of the mixing layer during the day.

7 Acknowledgements

The authors would like to thank the Municipality of Modena for providing traffic simulation data and Arpae Emilia-Romagna for providing data of and information pertaining to the traffic measurement campaign.

8 References

Bigi, A., Ghermandi, G., Harrison, R. M., 2012: Analysis of the air pollution climate at a background site in the Po Valley. *Journal of Environmental Monitoring*, 2012, 14, 552-563, https://doi.org/10.1039/c1em10728c.

Bigi, A. and Ghermandi, G., 2016: Trends and variability of atmospheric $PM_{2.5}$ and $PM_{10–2.5}$ concentration in the Po Valley, Italy, Atmos. Chem. Phys., 16, 15777-15788, https://doi.org/10.5194/acp-16-15777-2016.

Bigi, A., Bianchi, F., De Gennaro, G., Di Gilio, A., Fermo, P., Ghermandi, G., Prévôt, A.S.H., Urbani, M, Valli, G., Vecchi, R., Piazzalunga, A., 2017: Hourly composition of gas and particle phase pollutants at a central urban background site in Milan, Italy. *Atmospheric Research*, 186, 83-94, https://doi.org/10.1016/j.atmosres.2016.10.025.

Bellasio, R., Bianconi, R., 2012: The LAPMOD modelling system for simulating atmospheric pollution in complex orography. *Ingegneria Ambientale*, vol. XLI, n. 6, 492-500.

Berchet, A., Zink, K., Oettl, D., Brunner, J., Emmenegger, L., and Brunner, D., 2017: Evaluation of high-resolution GRAMM–GRAL (v15.12/v14.8) NOx simulations over the city of Zürich, Switzerland. Geosci. Model Dev., 10, 3441-3459, https://doi.org/10.5194/gmd-10-3441-2017.

Bove, M.C., Brotto, P., Cassola, F., Cuccia, E., Massabò, D., Mazzino, A., Piazzalunga, A., Prati, P., 2014: An integrated PM2.5 source apportionment study: positive Matrix Factorisation vs. the chemical transport model CAMx. Atmos. Environ. 94, 274–286, https://doi.org/10.1016/j.atmosenv.2014.05.039.

Carlino, G., Pallavidino, L., Prandi, R., Avidano, A., Matteucci, G., Ricchiuti, F., Bajardi, P., Bolognini, L., 2016: Micro-scale modelling of urban air quality to forecast NO_2 critical levels in traffic hot-spots. 10th *International Conference on Air Quality*, Milano, Italy.

Caserini, S., Pastorello, C., Gaifami, P., Ntziachristos, L., 2013: Impact of the dropping activity with vehicle age on air pollutant emissions. *Atmospheric Pollution Research*, vol. 4, 282-289, https://doi.org/10.5094/APR.2013.031.

Chang, J. and Hanna, S., 2004: Air quality model performance evaluation. *S. Meteorol Atmos Phys*, 87: 167, https://doi.org/10.1007/s00703-003-0070-7.

Chen, F., and Dudhia, J., 2001: Coupling an advanced land-surface/hydrology model with the Penn State/NCAR MM5 modeling system, Part I: Model description and implementation, Mon. Weather Rev., 557129, 569-585, https://doi.org/10.1175/1520-0493(2001)129<0569:CAALSH>2.0.CO;2.

Cimorelli, A.J., Perry, S. G., Venkatram, A., Weil, J. C., Paine, R. J., Wilson, R. B., Lee, R. F., Peters, W. D., and Brode, R. W., 2004: AERMOD: A dispersion model for industrial source applications Part I: General model formulation and boundary layer characterization. *J.Appl.Meteor*, https://doi.org/10.1175/JAM2227.1.

de Meij, A. and Gzella, A. and Cuvelier, C. and Thunis, P. and Bessagnet, B. and Vinuesa, J. F. and Menut, L. and Kelder, H. M., 2009: The impact of MM5 and WRF meteorology over complex terrain on CHIMERE model calculations. Atmos. Chem. Phys., 9, 6611-6632, https://doi.org/10.5194/acp-9-6611-2009.

Emmons, L.K., Walters, S., Hess, P. G., Lamarque, J.-F., Pfister, G.G., Fillmore, D., Granier, C., Guenther, A., Kinnison, D., Laepple, T., Orlando, J., Tie, X., Tyndall, G., Wiedinmyer, C., Baughcum, S. L., and Kloster, S., 2010: Description and evaluation of the Model for Ozone and Related chemical Tracers, version 4(MOZART-4), Geosci. Model Dev., 3, 43–67, https://doi.org/10.5194/gmd-3-43-2010.

European Environment Agency, 2011: The application of models under the European Union's Air Quality Directive: A technical reference guide, https://doi.org/10.2800/80600 technical report 10/2011.

European Environment Agency, 2016. Air quality in Europe – 2016 report.

Ghermandi, G., Tegi, S., Fabbi, S., Bigi, A., Zaccanti, M.M., 2014: Trigeneration power plant and conventional boilers: pollutant flow rate and atmospheric impact of stack emissions. *Int. Journal Environ. Science and Technology*, **12** (2): 693-704, https://doi.org/10.1007/s13762-013-0463-1.

Ghermandi, G., Fabbi, S., Zaccanti, M. M., Bigi A., Teggi, S., 2015: Micro–scale simulation of atmospheric emissions from power–plant stacks in the Po Valley. *Atmospheric Pollution Research*, **6**, 382-388, https://doi.org/10.5094/APR.2015.042.

Ghermandi, G., Fabbi, S., Bigi, A., Veratti, G., Despini, F., Teggi, S., Barbieri, C., Torreggiani, L., 2019: Impact assessment of vehicular exhaust emissions by microscale simulation using automatic traffic flow measurements. Atmospheric Pollution Research, https://doi.org/10.1016/j.apr.2019.04.004.

Gowardhan, A.A., Pardyjak, E.R., Senocak, I., Brown, M.J., 2011: A CFD based wind solver for an urban fast response transport and dispersion model. Environ. Fluid Mech. 11, 439–464, https://doi.org/10.1007/s10652-011-9211-6.

Grell, G.A., Peckham, S.E., Schmitz, R., McKeen, S.A., Frost, G., Skamarock, W.C., and Eder, B., 2005: Fully coupled "online" chemistry within the WRF model, Atmos. Environ., 39, 6957–6975, https://doi.org/10.1016/j.atmosenv.2005.04.027.

Grell, G.A. and Freitas, S.R., 2014: A scale and aerosol aware stochastic convective parameterization for weather and air quality modeling, Atmos. Chem. Phys., 14, 5233-5250, https://doi.org/10.5194/acp-14-5233-2014.

Gsella, A., de Meij, A., Kerschbaumer, A., Reimer, E., Thunis, P., Cuvelier, C., 2014: Evaluation of MM5, WRF and TRAMPER meteorology over the complex terrain of the Po Valley, Italy. Atmospheric Environment, 89, 797-806, https://doi.org/10.1016/j.atmosenv.2014.03.019.

826 Guenther, A.B., Jiang, X., Heald, C.L., Sakulyanontvittaya, T., Duhl, T., Emmons, L.K., and Wang, X., 2012: The Model of
827 Emissions of Gases and Aerosols from Nature version 2.1 (MEGAN2.1): an extended and updated framework for
828 modeling biogenic emissions, Geosci. Model Dev., 5, 1471-1492, https://doi.org/10.5194/gmd-5-1471-2012.
829 Hanna, S.R., Briggs, G.A., Hosker, Jr R.P., 1982: Handbook on atmospheric diffusion. Atmospheric Turbulence and
830 Diffusion Lab, National Oceanic and Atmospheric Administration, Oak Ridge, Tennessee, USA. Tech Rep
831 DOE/TIC-1122
832 Hanna, S.R., Chang, J.C., 2012: Acceptance criteria for urban dispersion model evaluation. Meteorological Atmospheric
833 Physics 116, 133–146, https://doi.org/10.1007/s00703-011-0177-1.
834 Hausberger, S., Matzer, C., Lipp, S., Weller, K., Dippold, M., Röck, M., Rexeis, M. and Silberholz, G., 2019: Consistent
835 Emission Factors from PEMS and Chassis Dyno Tests for HBEFA 4.1; TAP Conference, Thessaloniki, Greece.
836 HBEFA, 2019, https://www.hbefa.net/e/index.html (last access 9 December 2019).
837 Hodzic, A. and Jimenez, J. L., 2011: Modeling anthropogenically controlled secondary organic aerosols in a megacity: a
838 simplified framework for global and climate models, Geosci. Model Dev., 4, 901-917, https://doi.org/10.5194/gmd-
839 4-901-2011.
840 Hong, S.-Y., 2010: A new stable boundary-layer mixing scheme and its impact on the simulated East Asia summer monsoon
841 Q. J. R. Meteorol. Soc., 136 (651) (2010), pp. 1481-1496, https://doi.org/10.1002/qj.665.
842 Ibarra-Espinosa, S., Ynoue, R., O'Sullivan, S., Pebesma, E., Andrade, M.D.F., Osses, M., 2018: VEIN v0.2.2: an R package
843 for bottom-up vehicular emissions inventories, Geosci. Model Dev., 11, 2209-2229, https://doi.org/10.5194/gmd-
844 11-2209-2018.
845 INEMAR, 2013, https://www.arpae.it/dettaglio_generale.asp?id=4094&idlivello=1691(last access 2 September 2019).
846 Kaplan, H., Dinar, N., 1996: A Lagrangian dispersion model for calculating concentration distribution within a built-up
847 domain. Atmos. Environ. 30 (24), 4197–4207
848 Kuenen, J.J.P., Visschedijk, A.J.H., Jozwicka, M., Denier Van Der Gon, H.A.C., 2014: TNO-MACC-II emission inventory;
849 A multi-year (2003-2009) consistent high-resolution European emission inventory for air quality modelling, Atmos.
850 Chem. Phys., 14, 10963-10976, https://doi.org/10.5194/acp-14-10963-2014.
851 Kuik, F., Lauer, A., Churkina, G., Denier van der Gon, H. A. C., Fenner, D., Mar, K. A., and Butler, T. M., 2016: Air quality
852 modelling in the Berlin–Brandenburg region using WRF-Chem v3.7.1: sensitivity to resolution of model grid and
853 input data, Geosci. Model Dev., 9, 4339-4363, https://doi.org/10.5194/gmd-9-4339-2016.
854 Kuik, F., Kerschbaumer, A., Lauer, A., Lupascu, A., von Schneidemesser, E. and Butler, T. M., 2018: Top--down
855 quantification of NO_x emissions from traffic in an urban area using a high-resolution regional atmospheric
856 chemistry model. Atmos. Chem. Phys. 18, 8203-8225, https://doi.org/10.5194/acp-18-8203-2018.
857 Kwak, K. H., Baik, J. J., Ryu, Y. H., & Lee, S. H., 2015: Urban air quality simulation in a high-rise building area using a
858 CFD model coupled with mesoscale meteorological and chemistry-transport models. Atmospheric Environment,
859 100, 167-177. https://doi.org/10.1016/j.atmosenv.2014.10.059
860 Lenschow, P., Abraham, H., Kutzner, K., Lutz, M., Preub, J., Reichenbacher, W., 2001: Some ideas about the sources of
861 PM10. Atmos Environ 35, S23-S33, https://doi.org/10.1016/S1352-2310(01)00122-4.
862 Lin, Y.-L., Farley, R. D., Orville, H. D., 1983: Bulk parameterization of the snow field in a cloud model, J. Climate Appl.
863 Meteor., 22, 1065-1092, https://doi.org/10.1175/1520-0450(1983)022<1065:BPOTSF>2.0.CO;2.
864 Loomis, D., Grosse, Y., Lauby-Secretan, B., El Ghissassi, F., Bouvard, V., Benbrahim-Tallaa, L., Guha, N., Baan, R.,
865 Mattock, H., Straif, K., 2013: The carcinogenicity of outdoor air pollution. 14, 1262-1263,
866 https://doi.org/10.1016/S1470-2045(13)70487-X.
867 Masiol, M., Benetello, F., Harrison, R. M., Formenton, G., De Gaspari, F., Pavoni, B., 2015: Spatial, seasonal trends and
868 transboundary transport of PM2.5 inorganic ions in the Veneto region (Northeastern Italy). Atmospheric
869 Environment, 117, 19-31, https://doi.org/10.1016/j.atmosenv.2015.06.044.
870 Malm, W.C., Collett Jr., J.L., Barna, M.G., Gebhart, K.A., Schichtel, B.A., Beem, K., Carrico, C.M., Day, D.E., Hand, J.L.,
871 Kreidenweis, S.M., Lee, T., Levin, E., McDade, C., McMeeking, G.R., Molenar, J.V., Raja, S., Rodriguez, M.A.,
872 Schwandner, F., Sullivan, A.P., Taylor, C., 2009: RoMANS Rocky Mountain Atmospheric Nitrogen and Sulfur
873 Study Report Appendix 2. MM5 Performance Evaluation and Quality Assurance Review for the White River Field
874 Office Ozone Assessment, URS Corporation, Denver.

Mar, K.A., Ojha, N., Pozzer, A., and Butler, T. M., 2016: Ozone air quality simulations with WRF-Chem (v3.5.1) over Europe: model evaluation and chemical mechanism comparison, Geosci. Model Dev., 9, 3699-3728, https://doi.org/10.5194/gmd-9-3699-2016.

Mlawer, E. J., Taubaman, S. J., Brown, P. D., Iacono, M. J., and Clough, S. A., 1997: Radiative transfer for inhomogeneous atmosphere: RRTM, a validate correlated-k model for the longwave, J. Geophys. Res., 102(D14),16663-16682, https://doi.org/10.1029/97JD00237.

Moussafir, J., Oldrini, O., Tinarelli, G., Sontowski, J., Dougherty, C., 2004: A new operational approach to deal with dispersion around obstacles: the MSS (Micro-Swift-Spray) software suite. 9th International Conference on Harmonisation within Atmospheric Dispersion Modelling for Regulatory Purposes Garmisch 1-4 June 2004.

Moussafir, J., Olry, C., Nibart, M., Albergel, A., Armand, P., Duchenne, C., Mahe, F., Thobois, L., Le Loaëc, S., Oldrini, O., 2013: Aircity: a very high-resolution 3d atmospheric dispersion modeling system for Paris. Proc. 15th International Conference on Harmonisation within Atmospheric Dispersion Modelling for Regulatory Purpose, Madrid, Spain, May 6-9, 2013.

Novaes, P., Hilário, P., do Nascimento, S., Matsuda, M., Macchione, M., Peres Rangel, M., Kara-José, N., Berra, A., 2010: The effects of chronic exposure to traffic derived air pollution on the ocular surface. 10, 372-374, https://doi.org/10.1016/j.envres.2010.03.003.

Ntziachristos, L., Samaras, Z., 2016: EMEP/Eea Emission Inventory Guidebook; Road Transport: Passenger Cars, Light Commercial Trucks, Heavy-Duty Vehicles Including Buses and Motorcycles. European Environment Agency, Copenhagen.

Oldrini, O., Olry, C., Moussafir, J., Armand, P., Duchenne, C., 2011: Development of PMSS, the Parallel Version of Micro SWIFT SPRAY. Proc. 14th Int. Conf. on Harmonisation within Atmospheric Dispersion Modelling for Regulatory Purposes, 443-447.

Oldrini, O., Armand, P., Duchenne, C., Olry, C., Tinarelli, G., 2017. Description and preliminary validation of the PMSS fast response parallel atmospheric flow and dispersion solver in complex built-up areas. J. Environ. Fluid Mech. 17 (3), 1–18, https://doi.org/10.1007/s10652-017-9532-1.

Oldrini, O., Armand, P., 2019: Validation and Sensitivity Study of the PMSS Modelling System for Puff Releases in the Joint Urban 2003 Field Experiment, P. Boundary-Layer Meteorol 171: 513, https://doi.org/10.1007/s10546-018-00424-1.

Öttl, D., 2015: Evaluation of the revised Lagrangian particle model GRAL against wind-tunnel and field experiments in the presence of obstacles. *Boundary-Layer Meteorol*, 155, 271-287, https://doi.org/10.1007/s10546-014-9993-4.

Pirovano, G., Colombi, C., Balzarini, A., Riva, G., Gianelle, V., Lonati, G., 2015: PM2.5 source apportionment in Lombardy (Italy): comparison of receptor and chemistry-transport modelling results. Atmos. Environ. 106, 56–70, https://doi.org/10.1016/j.atmosenv.2015.01.073.

PopeIII, C. A., Burnett, R.T., Thurston, G. D., Thun, M. J., Calle, E. E., Krewski, D., Godleski, J. J., 2003: Cardiovascular Mortality and Long-Term Exposure to Particulate Air Pollution. Epidemiological Evidence of General Pathophysiological Pathways of Disease. 109, 71–77, https://doi.org/10.1161/01.CIR.0000108927.80044.7F.

Röckle, R., 1990. Bestimmung der Strömungsverhältnisse im Bereich komplexer Bebauungsstrukturen. PhD dissertation, (Darmstadt, Germany).

Rodean, H.C., 1996: Stochastic Lagrangian Models of Turbulent Diffusion, vol 45, American Meteorological Society, Boston, USA.

Sjödin, A, Borken-Kleefeld, J., Carslaw, D., Tate, J., Alt, G.-M., De la Fuente, J., Bernard, Y., Tietge, U., McClintock, P., Gentala, R., Vescio, N., Hausberger, S., 2018: Real-driving emissions from diesel pas-senger cars measured by remote sensing and as compared with PEMS and chassis dynamometer measurements -CONOX Task 2 report; Commissioned by the Federal Office for the Environment (FOEN), Switzerland; ISBN: 978-91-88319-70-8.

Tewari, M, Kusaka, H., Chen, F., Coirier, W.J., Kim, S., Wyszogrodzki, A.A., Warner, T.T., 2010: Impact of coupling a microscale computational fluid dynamics model with a mesoscale model on urban scale contaminant transport and dispersion. Atmos. Res., 96 , 656-664. https://doi.org/10.1016/j.atmosres.2010.01.006

Thomson, D.J., 1987. Criteria for the selection of stochastic models of particle trajectories in turbulent flows. J. Fluid Mech. 180, 529–556, https://doi.org/10.1017/S0022112087001940.

Thunis, P., Triacchini, G., White, L., Maffeis, G., Volta, M., 2009: Air pollution and emission reductions over the Po-Valley: Air quality modelling and integrated assessment. 18th World IMACS / MODSIM Congress, Cairns, Australia 13-17 July, p. 2009 2335-2341.

Thunis, P., 2018: On the validity of the incremental approach to estimate the impact of cities on air quality. Atmos. Environ. 173, 210-222, https://doi.org/10.1016/j.atmosenv.2017.11.012.

Tinarelli, G., Giostra, U., Ferrero, E., Tampieri, F., Anfossi, D., Brusasca, G., Trombetti, F., 1992: SPRAY, a 3-D particle model for complex terrain dispersion", Proc. of 10th Symposium on Turbulence and Diffusion, American Meteorological Society, Portland, Oregon (USA), 29-Sept. 2-Oct, P2.9, 147-150.

Tinarelli, G., Brusasca, G., Oldrini, O., Anfossi, D., Trini Castelli, S., Moussafir, J., 2007: Micro-SWIFT-SPRAY (MSS): a new modelling system for the simulation of dispersion at microscale. General description and validation. In: Air Pollution Modeling and its Application XVII. Springer International Publishing, pp. 449–458449–458, https://doi.org/10.1007/978-0-387-68854-1_49.

Tinarelli, G., Mortarini, L., Trini Castelli, S., Carlino, G., Moussafir, J., Olry, C., Armand, P., Anfossi, D., 2013: Review and validation of Micro-Spray, a Lagrangian particle model of turbulent dispersion. *Geophysical monograph*, American Geophysical Union (AGU), vol 200, pp 311–327, https://doi.org/10.1029/2012GM001242.

Tositti, L., Brattich, E., Masiol, M., Baldacci, D., Ceccato, D., Parmeggiani, S., Stracquadanio, M., Zappoli, S., 2014: Source apportionment of particulate matter in a large city of southeastern Po Valley (Bologna, Italy). Environ. Sci. Pollut. Control Ser. 21 (2), 872–890, https://doi.org/10.1007/s11356-013-1911-7.

Trini Castelli, S., Tinarelli, G., Reisin, T.G., 2017: Comparison of atmospheric modelling systems simulating the flow, turbulence and dispersion at the microscale within obstacles. Environ. Fluid Mech. 17, 879–901, https://doi.org/10.1007/s10652-017-9520-5.

Trini Castelli, S., Armand, P., Tinarelli, G., Duchenne, C., Nibart, M., 2018: Validation of a Lagrangian particle dispersion model with wind tunnel and field experiments in urban environment. *Atmospheric Environment*, 193, 273-289, https://doi.org/10.1016/j.atmosenv.2018.08.045.

Wyszogrodzki, A.A., Miao, S., Chen, F., 2012: Evaluation of the coupling between mesoscale-WRF and LES-EULAG models for simulating fine-scale urban dispersion, Atmos. Res., 118, 324-345. https://doi.org/10.1016/j.atmosres.2012.07.023

Zaveri, R.A., Easter, R. C., Fast, J. D., and Peters, L. K., 2008: Model for Simulating Aerosol Interactions and Chemistry (MOSAIC), *J. Geophys. Res.*, 113, D13204, https://doi.org/10.1029/2007JD008782.